Peyer's patch myeloid cells infection by Listeria signals through gp38 + stromal cells and locks intestinal villus invasion

Olivier Disson, Camille Bleriot, Jean-Marie Jacob, Nicolas Serafini, Sophie Dulauroy, Grégory Jouvion, Cindy Fevre, Grégoire Gessain, Pierre Thouvenot, Gérard Eberl, et al.

JEM Journal of Experimental Medicine

ARTICLE

Peyer's patch myeloid cells infection by *Listeria* signals through gp38$^+$ stromal cells and locks intestinal villus invasion

Olivier Disson[1,2], Camille Blériot[1,2]*, Jean-Marie Jacob[3,4]*, Nicolas Serafini[5,6]*, Sophie Dulauroy[4,7], Grégory Jouvion[8], Cindy Fevre[1,2], Grégoire Gessain[1,2], Pierre Thouvenot[1,2], Gérard Eberl[4,7], James P. Di Santo[5,6], Lucie Peduto[3,4], and Marc Lecuit[1,2,9]

The foodborne pathogen *Listeria monocytogenes* (*Lm*) crosses the intestinal villus epithelium via goblet cells (GCs) upon the interaction of *Lm* surface protein InlA with its receptor E-cadherin. Here, we show that *Lm* infection accelerates intestinal villus epithelium renewal while decreasing the number of GCs expressing luminally accessible E-cadherin, thereby locking *Lm* portal of entry. This novel innate immune response to an enteropathogen is triggered by the infection of Peyer's patch CX3CR1$^+$ cells and the ensuing production of IL-23. It requires STAT3 phosphorylation in epithelial cells in response to IL-22 and IL-11 expressed by lamina propria gp38$^+$ stromal cells. *Lm*-induced IFN-γ signaling and STAT1 phosphorylation in epithelial cells is also critical for *Lm*-associated intestinal epithelium response. GC depletion also leads to a decrease in colon mucus barrier thickness, thereby increasing host susceptibility to colitis. This study unveils a novel innate immune response to an enteropathogen, which implicates gp38$^+$ stromal cells and locks intestinal villus invasion, but favors colitis.

Introduction

The intestinal epithelium directly interacts with the external environment and is constantly renewed by stem cells located in intestinal crypts (Barker, 2014). The maintenance of intestinal epithelial homeostasis is tightly regulated by pericryptal stromal cells (Stzepourginski et al., 2017) and the sensing of microbe-associated molecular patterns (MAMPs) from the microbiota (Rakoff-Nahoum et al., 2004; Sommer and Bäckhed, 2013).

Most invasive enteropathogens disrupt gut homeostasis: they can directly modulate epithelial proliferation by inhibiting cell cycle, as does *Shigella flexnerii* IpaB, which acts on Mad2L2 (Iwai et al., 2007), or promote it, as does the gastric carcinogen *Helicobacter pylori* (Mimuro et al., 2002). *Salmonella enterica*, *S. flexnerii*, and attaching and effacing bacteria such as *Citrobacter rodentium*, which are all associated with enteritis, lead to epithelial barrier disruption and intestinal inflammation (Sansonetti et al., 1999; Collins et al., 2014). *C. rodentium*–associated epithelial damage leads to MyD88-dependent epithelial proliferation (Gibson et al., 2008). In a *Drosophila melanogaster* model of intestinal infection, epithelial proliferation is the consequence of the immune oxidative burst and is JAK/STAT dependent (Buchon et al., 2009). This phenotype is mediated by signaling from the damaged epithelium to stem cells and amplified by visceral muscles (Buchon et al., 2013). In noninfectious models of dextran sodium sulfate (DSS)–induced colitis and methotrexate-induced damage to stem cells, intestinal epithelium wound healing depends on intestinal epithelial cell STAT3 activation by IL-22 (Pickert et al., 2009; Aparicio-Domingo et al., 2015). Upon *C. rodentium* infection, IL-23 expression by CX3CR1$^+$ cells triggers IL-22 expression by type 3 innate lymphoid cells (ILCs; Longman et al., 2014; Aychek et al., 2015). It has also been shown that IL-22 acts on enterocytes in a STAT3-dependent manner, inducing RegIIIβ and RegIIIγ expression (Zheng et al., 2008; Manta et al., 2013). Epithelial renewal upon infectious- and noninfectious-associated damages may therefore engage the same signaling.

The intestinal phase of listeriosis, a systemic infection caused by the foodborne pathogen *Listeria monocytogenes* (*Lm*), is mostly asymptomatic (Charlier et al., 2017), in line with the observation that *Lm* does not significantly alter the intestinal barrier integrity

[1]Institut Pasteur, Biology of Infection Unit, Paris, France; [2]Institut National de la Santé et de la Recherche Médicale U1117, Paris, France; [3]Institut Pasteur, Stroma, Inflammation and Tissue Repair Unit, Paris, France; [4]Institut National de la Santé et de la Recherche Médicale U1224, Paris, France; [5]Institut Pasteur, Innate Immunity Unit, Paris, France; [6]Institut National de la Santé et de la Recherche Médicale U1223, Paris, France; [7]Institut Pasteur, Microenvironnement and Immunity Unit, Paris, France; [8]Institut Pasteur, Human Histopathology and Animal Models Unit, Paris, France; [9]Paris Descartes University, Department of Infectious Diseases and Tropical Medicine, Necker-Enfants Malades University Hospital, APHP, Institut Imagine, Paris, France.

*C. Blériot, J.-M. Jacob, and N. Serafini contributed equally to this paper; Correspondence to Marc Lecuit: marc.lecuit@pasteur.fr; C. Blériot's present address is Singapore Immunology Network, Agency for Science, Technology, and Research, Singapore.

(Lecuit et al., 2007; Tsai et al., 2013). *Lm* has the ability to enter epithelial cells through interaction of its surface protein InlA with its receptor E-cadherin (Ecad). As InlA–Ecad interaction is species specific, we generated transgenic (hEcad) and knock-in (KIE16P) humanized Ecad mouse lines to study listeriosis in vivo (Lecuit et al., 2001; Disson et al., 2008). In humanized Ecad mice, *Lm* is rapidly transcytosed at the small intestinal level in an InlA–Ecad-dependent manner across goblet cells (GCs) expressing luminally accessible Ecad and released into the lamina propria (LP; Fig. S1 A; Lecuit et al., 2001; Nikitas et al., 2011). *Lm* is also transferred, albeit at a lower efficiency, through M cells in an InlA-independent manner at the Peyer's patch (PP) level, the only route of infection in nonhumanized mice (Jensen et al., 1998; Chiba et al., 2011; Gessain et al., 2015). We have shown by transcriptomic analysis that the global intestinal host response to *Lm* is InlA independent and triggered by invasion of PPs (Fig. S1 A; Lecuit et al., 2007). It requires the expression of listeriolysin O (LLO; Lecuit et al., 2007), a major *Lm* virulence factor involved in *Lm* escape from its phagocytic vacuole and survival in professional phagocytes (Hamon et al., 2012). We have also shown that *Lm* induces IL-22 and IFN-γ upon oral infection in humanized Ecad mice (Reynders et al., 2011). Whereas IFN-γ is required to control systemic *Lm* infection (Harty and Bevan, 1995), IL-22 is not (Graham et al., 2011).

Lm impact on intestinal epithelium homeostasis, although potentially critical for the outcome of the infection, has not been studied. We therefore investigated intestinal epithelium response to orally acquired listeriosis. We show here that *Lm* induces intestinal epithelial cell proliferation and depletion of GCs expressing accessible Ecad, leading to a complete blockade of *Lm* intestinal villus invasion. Intestinal epithelium proliferation and GC depletion are independent of *Lm* intestinal villus invasion, but strictly depend on infection of PP CX3CR1$^+$ cells, which express IL-23 upon infection, leading to STAT3 activation in enterocytes. However, in contrast to host responses to intestinal epithelial damage, *Lm*-associated IL-23–dependent STAT3 phosphorylation involves not only IL-22 expression, but also induction of IL-11 by LP CD45$^-$ gp38$^+$ pericryptal stromal cells. Importantly, we show that IL-23/IL-22/IL-11–dependent intestinal epithelium response to *Lm* also critically requires IFN-γ–dependent STAT1 phosphorylation. We further demonstrate that this innate immune pathway leads to a decrease of mucus barrier thickness at the colon level, a known promoter of intestinal inflammation (Van der Sluis et al., 2006). Indeed, *Lm*-associated epithelial response leads to gut sensitization to colitis.

Altogether, these results identify a new innate immune pathway initiated at the PP level against infection, which relies on IL-22– and IL-11–dependent STAT3 activation in epithelial cells and the conjugated action of IFN-γ. This study unveils a new layer of regulation of the intestinal epithelium in response to invasive pathogens and the unexpected role of LP CD45$^-$ gp38$^+$ CD34$^+$ stromal cells as innate immune cells responding to pathogen-elicited stimuli.

Results

Lm infection leads to intestinal epithelium proliferation

We first investigated intestinal epithelium proliferation upon *Lm* oral inoculation by quantifying BrdU incorporation in KIE16P humanized mouse intestinal epithelium. Whereas only cells located in intestinal crypts incorporated BrdU at steady-state (Barker et al., 2008), oral infection with two genetically distant WT *Lm* strains (EGD and EGDe) induced a significant increase in BrdU$^+$ epithelial cells (Fig. 1 A and Fig. S1 B). Increase in enterocyte BrdU incorporation was noticeable as early as day 2 post infection (pi). As BrdU was injected i.p. and incorporated in dividing cells 16 h before tissue sampling, this indicates that proliferation begins in the first day pi. Proliferation peaked between day 3 and 4 pi and returned to basal level at day 6 pi (Fig. 1 B). In line with these results, more Ki67$^+$ cycling cells were counted in crypts and at crypt-villous junctions upon *Lm* oral infection (Fig. 1 C and Fig. S1 C; Whitfield et al., 2006; Cuylen et al., 2016). No leakage of the epithelial barrier was detected in a biotin barrier assay (Fig. S1 D; Tsai et al., 2013), and no induction of epithelial cell death was observed (Fig. S1 E). We next investigated the dose-dependency of *Lm*-associated enterocyte proliferation. Epithelial proliferation was induced similarly upon oral inoculation of 5×10^8 and 5×10^9 CFUs, but not 5×10^7 CFUs/animal (Fig. S1 F).

Lm-associated intestinal epithelium proliferation is independent of villus epithelial cell invasion, but requires PP infection

We next investigated the bacterial determinants of intestinal epithelial proliferation. Since *Lm* crosses the villus intestinal epithelial barrier in an InlA-dependent manner (Fig. S1 A), we investigated if cell proliferation was dependent of InlA-mediated villus invasion. Enterocyte proliferation was detected in all intestinal crypts observed, irrespective of local *Lm* villus invasion, while only 10% of villi are infected (Fig. S1 G). This argues against local proliferation in response to InlA-dependent infection of villi. To directly investigate the role of InlA-dependent villus invasion in *Lm*-associated intestinal epithelium proliferation, KIE16P humanized mice were infected with an isogenic *Lm* Δ*inlA* mutant, which is unable to invade intestinal villi, but crosses via PPs. As expected, intestinal bacterial load was lower upon infection with *Lm* Δ*inlA* as compared with WT bacteria (Fig. S1 H). Nevertheless, *Lm*-associated intestinal epithelium proliferation was comparable in both conditions (Fig. 1, D and E). As previously shown, *Lm* invades via M cells in an InlA-independent manner the PP (Lecuit et al., 2001; Chiba et al., 2011; Nikitas et al., 2011), where host response to *Lm* is initiated (Fig. 1 F and Fig. S1 A; Lecuit et al., 2007). To investigate the role of PPs in *Lm*-associated intestinal epithelium proliferation, we injected *Lm* Δ*inlA* in ligated loops containing or not containing a PP. *Lm*-associated intestinal epithelium proliferation was strictly dependent of the presence of PPs (Fig. 1 G), demonstrating the critical role of PPs in *Lm*-associated intestinal epithelium proliferation and the absence of contribution of InlA-dependent invasion in this phenomenon. Of note, proliferation was higher in villi near to PPs, suggesting a gradient of induction from PP to LP (Fig. S1 I). We confirmed that proliferation is InlA-independent in nonhumanized C57BL/6J mice, in which *Lm* entry occurs only through PP M cells (Fig. S1 J).

As intestinal proliferation is regulated by the microbiota (Rakoff-Nahoum et al., 2004), we investigated whether *Lm*-associated intestinal epithelium proliferation was indirect, as a

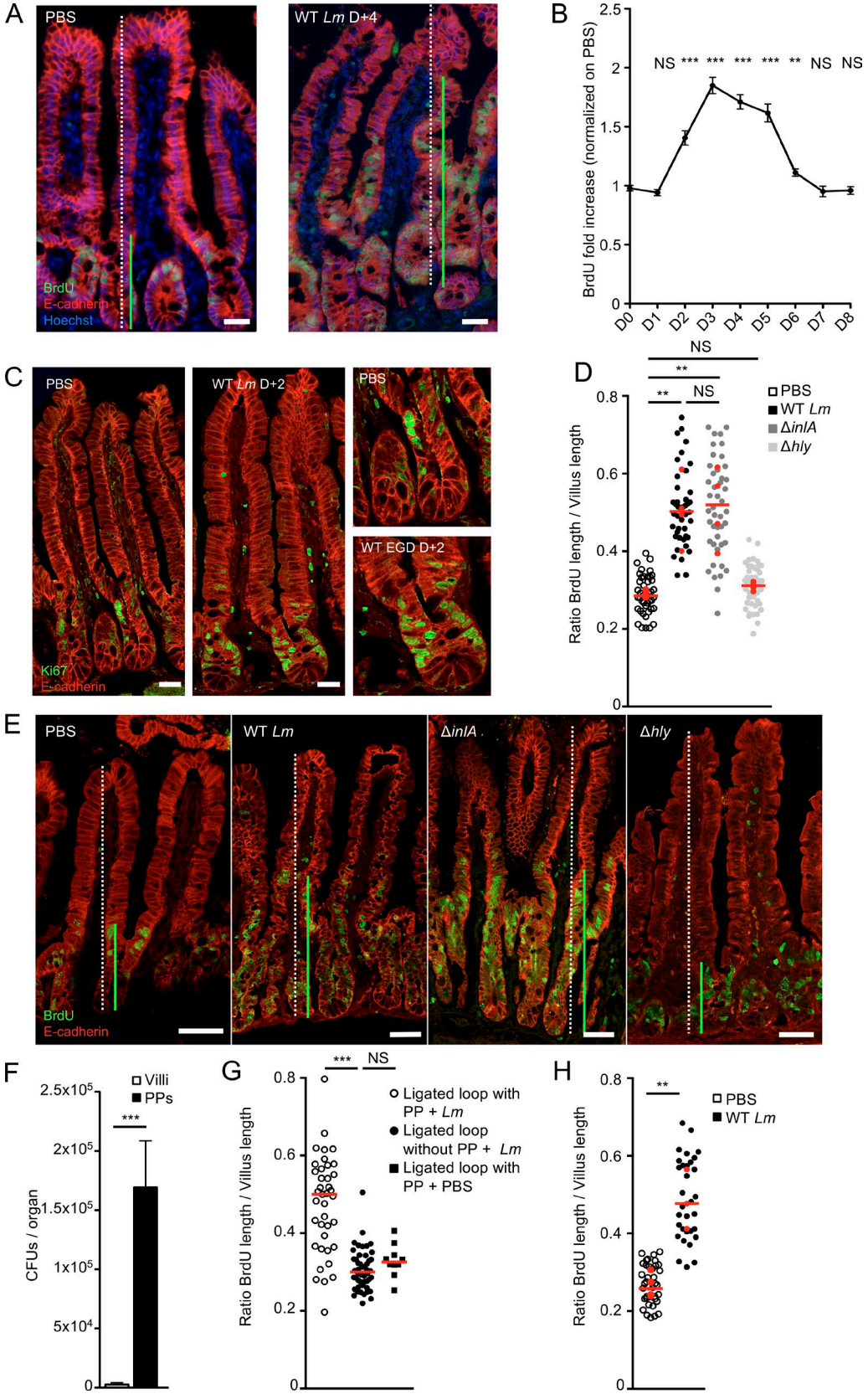

Figure 1. ***Lm*-induced epithelial cell proliferation in an InlA-independent but PP-dependent manner. (A)** Fluorescent imaging of sections of the ileum obtained from KIE16P mice 4 d after oral infection with 5×10^9 *Lm*. 16 h before euthanasia, mice were injected with BrdU. Sections are stained for proliferating cells (BrdU), epithelial cells (Ecad), and nuclei (Hoechst). Bars, 20 µm. **(B)** Quantification over time of epithelial proliferation. Fold increase is measured by dividing the length between the first and last BrdU$^+$ epithelial cells by the length of the villi, normalized by the proliferation from the noninfected mice. $n = 9–39$

consequence of an interaction with the microbiota. As in conventional mice, proliferation was induced in germ-free mice mono-associated with *Lm*, demonstrating the direct impact of *Lm* on proliferation, rather than via interactions with the microbiota (Fig. 1 H).

Lm-associated intestinal epithelium proliferation depends on epithelial STAT3 activation and leads to a blockade of *Lm* intestinal villus invasion via GCs

STAT3 activation leads to epithelial cell proliferation upon DSS-induced colitis and methotrexate-induced damage to stem cells (Pickert et al., 2009; Aparicio-Domingo et al., 2015). We generated and infected nonhumanized C57BL/6J *Stat3*$^{fl/fl}$ *vil-Cre-ER*^{T2} mice, in which *Stat3* is excised in intestinal epithelial cells (IEC) expressing Villin by hydroxytamoxifen. Proliferation was totally impaired in STAT3$^{IEC\text{-}KO}$ mice as compared with STAT3$^{IEC\text{-}WT}$ littermates, demonstrating the critical role of epithelial STAT3 in *Lm*-associated intestinal epithelium proliferation, independently of InlA-dependent entry (Fig. 2, A and B). GCs expressing accessible Ecad are the main sites of InlA-dependent *Lm* translocation across the intestinal epithelium (Nikitas et al., 2011). Since STAT3-dependent epithelial proliferation may be linked to the turnover and differentiation of GCs (Gonneaud et al., 2016), we investigated the impact of *Lm*-associated intestinal epithelium proliferation on GCs. We labeled Muc2, the major component of mucin synthesized by GCs, with an anti-MUC2C3 antibody (Johansson et al., 2008). We also stained glycosylated mucins with wheat germ agglutinin (WGA), which specifically binds to sialic acid and N-acetyl-glucosaminyl carbohydrate residues on mature, modified mucins (Fischer et al., 1984). The number of WGA$^+$ Muc2$^+$ GCs was significantly decreased in intestinal villi from infected mice as early as 1 d pi and recovered 14 d pi (Fig. 2, C and D; and Fig. S2 A). The decrease in WGA$^+$ GC number was STAT3-dependent, as excision of STAT3 in *Stat3*$^{fl/fl}$ *vil-Cre-ER*^{T2} mice prevented *Lm*-induced decrease in GC number (Fig. 2 E and Fig. S2 B). As for proliferation, WGA$^+$ GC number regulation was InlA independent (Fig. S2 C). We next investigated the expression of Muc2 in GCs. Unlike the clear decrease of WGA$^+$ GCs, the number of total Muc2$^+$ GC only slightly decreased in intestine (Fig. 2, D and F). Data from literature indicate that GCs that harbor less glycosylated mucins are not fully mature (Asker et al., 1998; Nowarski et al., 2015). We therefore investigated if the decrease in WGA$^+$ GCs may correlate with other markers of GC differentiation. We have shown previously that WGA$^+$ GCs express luminally accessible Ecad, which is targeted by *Lm* (Nikitas et al., 2011). We observed a dramatic STAT3-dependent decrease of WGA$^+$ GCs expressing accessible Ecad upon *Lm* infection (Fig. 2, G and H).

We next investigated the impact of decreased accessible Ecad on *Lm* InlA-dependent villus invasion. We generated humanized Ecad KIE16P STAT3$^{IEC\text{-}KO}$ and STAT3$^{IEC\text{-}WT}$ mice in which InlA-dependent entry occurs. To this end, we inoculated these mice with WT or *Lm* Δ*inlA* at 5 × 10^8 CFUs to activate STAT3. As expected, proliferation was inhibited in KIE16P STAT3$^{IEC\text{-}KO}$ compared with KIE16P STAT3$^{IEC\text{-}WT}$ (Fig. S2 D). 3 d later, we reinoculated with the same bacteria at higher dose of 5 × 10^9 CFUs for 4 d. Strikingly, InlA-dependent *Lm* entry was fully inhibited in KIE16P STAT3$^{IEC\text{-}WT}$ mice, whereas it was not in KIE16P STAT3$^{IEC\text{-}KO}$, showing that *Lm* infection blocks subsequent InlA-dependent entry in a STAT3-dependent manner (Fig. 2 I, middle). In sharp contrast, no impact was detected on translocation of *Lm* Δ*inlA*, suggesting that STAT3 activation inhibits specifically InlA-dependent entry that occurs via GCs (Fig. 2 I, right). As a control, we infected nonhumanized C57BL/6 STAT3$^{IEC\text{-}KO}$ and STAT3$^{IEC\text{-}WT}$ mice (Fig. 2 I, left) and confirmed that STAT3 has no impact on InlA-independent invasion, whereas proliferation and the number of WGA$^+$ GCs are modulated in these mice.

Together, these results indicate that STAT3 activation, which is induced by *Lm* in an InlA-independent manner, leads to a complete blockade of InlA-dependent intestinal villus invasion, by depleting specifically GCs expressing luminally accessible Ecad.

Infection of PP CX3CR1 initiates *Lm*-associated intestinal epithelium response

We next investigated how STAT3 is activated in the epithelium upon *Lm* infection in an InlA-independent but PP-dependent manner. We observed that *Lm* is rapidly captured mostly by CX3CR1$^+$ cells in PPs upon oral infection with 5 × 10^9 CFUs, whereas no bacteria was detected in PPs with 5 × 10^7 CFUs, which fits with the inoculum required for enterocyte proliferation (Fig. 3 A and Fig. S2, E and G). We next investigated the role of PP CX3CR1 in *Lm*-associated intestinal epithelium response. When compared with *Cx3cr1*$^{GFP/+}$ littermates, *Lm*-associated epithelial cell proliferation in *Cx3cr1*$^{GFP/GFP}$ mice was totally abolished (Fig. 3 B), even though *Lm* were present in both CX3CR1$^{GFP/+}$ and CX3CR1$^{GFP/GFP}$ cells (Fig. 3 A and Fig. S2 F). This indicates that CX3CR1 expression is critically needed for *Lm*-associated intestinal epithelium proliferation. Proliferation of epithelial cells and WGA$^+$ cell decrease required expression of LLO, which is encoded by *hly* and is necessary for bacterial escape from phagocytic vacuole (data

villi/point. Data are pooled from three independent experiments. Mann-Whitney test. **(C)** Confocal imaging of sections of the ileum obtained from KIE16P mice 2 d after oral infection with 5 × 10^9 *Lm*. Sections are stained for proliferating cells (Ki67) and epithelial cells (Ecad). Bars, 20 µm. **(D)** Quantification of epithelial proliferation in KIE16P littermate mice infected with 5 × 10^9 *Lm* and isogenic mutants. Each dot corresponds to one quantified villus, except the red dots, which correspond to the mean of each mouse. At least 5 fields/10 villi per mouse. *n* = 4 mice/bacterial strain. Data are pooled from two independent experiments. A one-way ANOVA test followed by a Sidak's multiple comparisons was performed on the mean of each mouse. **(E)** Confocal imaging of frozen sections of the ileum obtained from KIE16P mice treated as in A with 5 × 10^9 *Lm* and isogenic mutants. Bars, 20 µm. **(F)** *Lm* burden in PPs and villi from mice infected by 5 × 10^9 CFUs Δ*inlA Lm*. Eight mice per group. Data are represented as mean ± SEM. Mann-Whitney test. **(G)** Quantification of epithelial proliferation in ligated loop of KIE16P mice containing one or no PP infected with 1 × 10^5 Δ*inlA Lm* 24 h pi. Each dot corresponds to one quantified villus. At least 5 fields/10 villi per mouse. *n* = 3–4 mice/condition. One for PP PBS control. Data are pooled from two independent experiments. A one-way ANOVA test followed by a Tukey's multiple comparisons was performed. **(H)** Quantification of epithelial proliferation in axenic KIE16P littermate mice infected with 5 × 10^9 *Lm*. Each dot corresponds to one quantified villus, except the red dots, which correspond to the mean of each mouse. *n* = 3–4 mice. Data are pooled from two independent experiments. A Student's *t* test was performed on the mean of each mouse. **, P < 0.01; ***, P < 0.001.

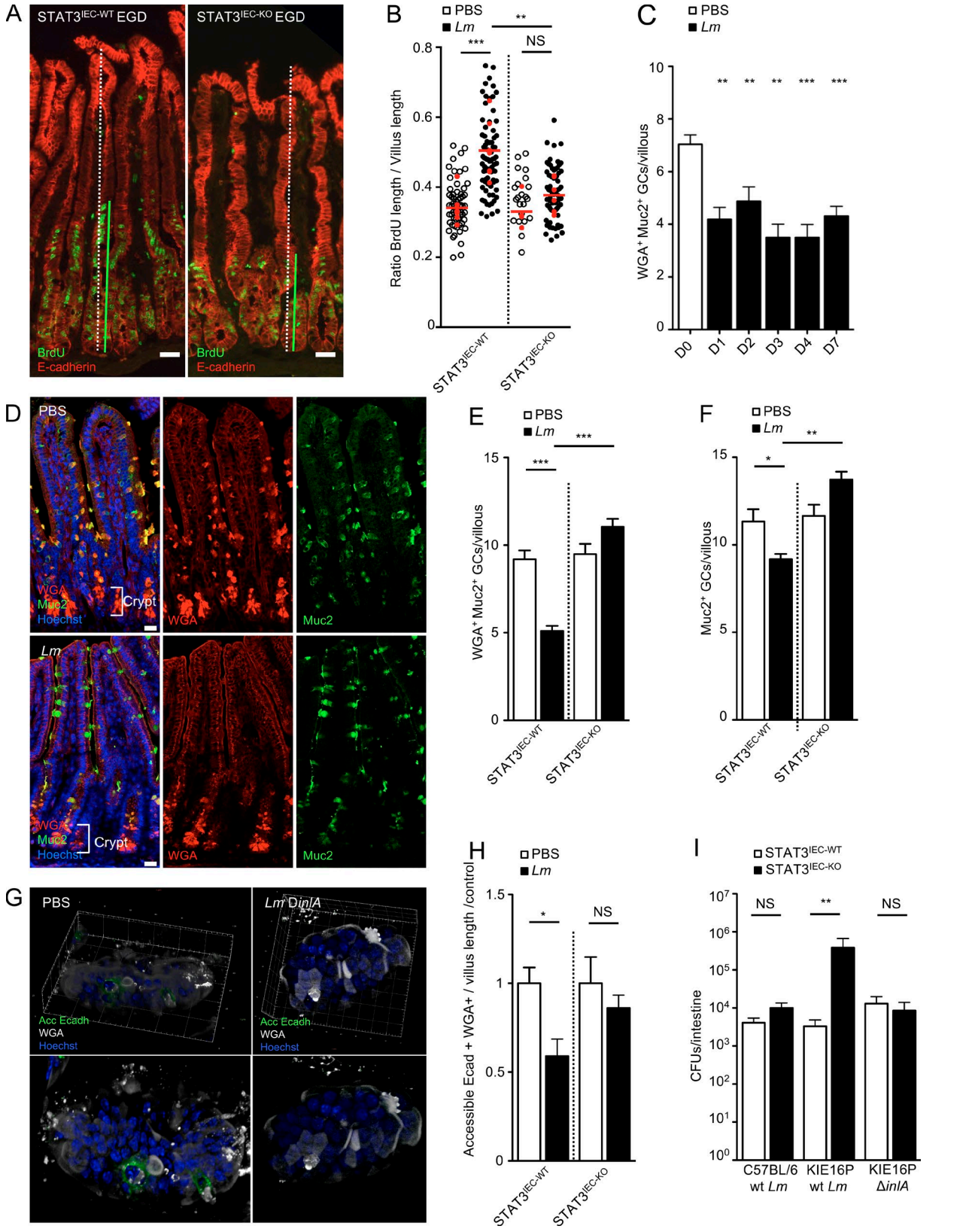

Figure 2. ***Lm* triggers a STAT3-dependent negative feedback loop blocking its access to intestinal villi via GCs. (A)** Confocal imaging of sections of the ileum obtained from STAT3^{IEC-WT} and STAT3^{IEC-KO} mice treated as in Fig. 1 A with 5 × 10^9 *Lm* and isogenic mutants. Bars, 20 µm. **(B)** Quantification of epithelial proliferation in STAT3^{IEC-WT} and STAT3^{IEC-KO} littermate mice 4 d after oral inoculation. Each dot corresponds to one quantified villus, except the red dots, which correspond to the mean of each mouse. *n* = 3–5 mice (PBS) or 6–7 mice (*Lm*)/condition. Data are pooled from three independent experiments. A one-way ANOVA test followed by a Sidak's multiple comparisons was performed on the mean of each mouse. **(C)** Quantification of WGA$^+$ GCs/villous at different time points after inoculation. *n* = 8–25 independent villi. Data are pooled from two independent experiments. Data are represented as mean ± SEM. Mann-Whitney test.

not shown). LLO is also required for *Lm*-associated intestinal epithelium proliferation in germ-free mice as well as in C57BL/6 mice, where entry occurs only via PPs (Fig. 1 H and Fig. S1 I). This suggests that *Lm* access to PP CX3CR1$^+$ cytoplasm is needed for signaling. We next investigated if PP CX3CR1$^+$ cells are involved in signaling upstream of STAT3. IL-23 and its downstream effector IL-22 are expressed in a CX3CR1-dependent manner upon *C. rodentium* infection (Longman et al., 2014; Aychek et al., 2015), and IL-22 is a potent inducer of epithelial proliferation (Pickert et al., 2009; Lindemans et al., 2015). We investigated if, as do colonic CX3CR1$^+$ cells upon *C. rodentium* infection, PP CX3CR1$^+$ cells express IL-23 upon *Lm* infection. At steady-state, most CX3CR1$^+$ cells were CX3CR1^{high} in PPs and villi, as previously reported (Varol et al., 2009; Bonnardel et al., 2015). However, upon 24 h of *Lm* oral infection, the number of CX3CR1^{int} mononuclear phagocytes (MPs) was significantly increased in PPs compared with noninfected tissue and villi from infected mice (Fig. 3 C). Upon infection, CX3CR1$^+$, and especially PP CX3CR1^{int} MPs, express *Il23* (Fig. 3 D and S2 H). We next showed that induction of *Il23p19* expression is CX3CR1-dependent in *Cx3cr1$^{GFP/GFP}$* mice (Fig. 3 E). These data demonstrate that CX3CR1 expression in PPs is necessary for IL-23 production in response to *Lm* infection.

We next investigated the role of IL-23 on *Lm*-associated intestinal epithelium proliferation. IL-23 pathway disruption in *Il23p19$^{-/-}$* mice fully impaired *Lm*-associated enterocyte proliferation (Fig. 3 F), indicating that IL-23, while being produced at the PP level, exerts its effect at the villus level. Surprisingly, enterocyte proliferation in response to *Lm* was still observed in *Il22$^{-/-}$* mice (Fig. 3 F). We therefore investigated whether other factors contributing to *Lm*-associated intestinal epithelium proliferation were involved and induced by IL-23. *Lm*-associated enterocyte proliferation was not abolished in *Rag2$^{-/-}$* mice, devoid of B and T cells, and was partially observed in *Rag2$^{-/-}$Il17ra$^{-/-}$* mice, which lack IL-17–induced signaling (Fig. 3 G). However, *Lm*-associated enterocyte proliferation was absent in *Rag2$^{-/-}$Il17ra$^{-/-}$* mice when treated with an anti–IL-22 antibody (Fig. 3 G), indicating that both IL-22 and IL-17 are involved in *Lm*-associated epithelial proliferation.

IL-11 expressed by gp38$^+$ stromal cells is involved in *Lm*-associated epithelial response

To decipher the complementary roles of IL-22 and IL-17 in *Lm*-associated epithelial response, we investigated the contribution of other modulators of epithelial proliferation potentially linked to IL-23 and STAT3. IL-11 is involved in gastric and colon tumorigenesis through STAT3 activation (Putoczki et al., 2013) and could therefore be a modulator of enterocyte proliferation. We first showed that *Il11* transcription is induced upon *Lm* infection in an IL-23–dependent manner (Fig. 4 A). We next showed that blocking of IL-22 in *Il11ra$^{-/-}$*mice fully inhibited proliferation, while blocking IL-11 or IL-22 alone is not sufficient (Fig. 3 F and Fig. 4 B). This indicates that both IL-11 and IL-22 contribute to IL-23–dependent *Lm*-associated enterocyte proliferation. We investigated the source of IL-11 during *Lm* infection. Several cell types in the intestinal LP have been reported to express IL-11, including immune cells, endothelial cells, and mesenchymal stromal cells (Bamba et al., 2003; Andoh et al., 2005; Putoczki and Ernst, 2010). We have previously shown that a majority of mesenchymal stromal cells of the LP, both in the villi and around the crypts, express gp38 (podoplanin; Peduto et al., 2009; Stzepourginski et al., 2015). CD45$^-$CD31$^-$gp38$^+$ stromal cells isolated from the LP of infected mice expressed significantly higher level of *Il11* transcripts compared with intestinal immune cells (CD45$^+$) and endothelial cells (CD31$^+$; Fig. 4 C and Fig. S3 A). Among total gp38$^+$ stromal cells, the pericryptal subset coexpressing CD34, which we previously identified as a major component of the intestinal stem cell niche (Stzepourginski et al., 2017), is the major source of IL-11 expression upon *Lm* infection (Fig. 4 C and Fig. S3 B). In vitro stimulation of gp38$^+$ stromal cells by recombinant IL-23 did not induce expression of IL-11 (Fig. 4 D), consistent with the observation that gp38$^+$ stromal cells do not express IL-23 receptor (Fig. S3 C). These results suggest that another factor bridges IL-23 signaling with IL-11 expression. Since IL-17 plays a role in *Lm*-associated enterocyte proliferation (Fig. 3 G), we investigated its contribution to gp38$^+$ stromal cells' IL-11 production. IL-17 was sufficient to increase IL-11 release by gp38$^+$ stromal cells (Fig. 4 D), indicating a role for IL-17 in IL-11 production.

We next investigated in vivo whether IL-11, IL-17, and IL-22 complement IL-23 inhibition to induce *Lm*-associated enterocyte proliferation. Treatment of *Lm*-infected *Il23p19$^{-/-}$* mice with recombinant IL-11, IL-17, or IL-22 fully restored *Lm*-associated epithelial proliferation, as well as a decrease in WGA$^+$ GCs (Fig. 4, E and F). Together, these results show that intestinal gp38$^+$ stromal cells are the major producer of IL-11 after *Lm* infection, which acts in concert with IL-22 downstream of IL-23 and IL-17 to induce *Lm*-associated intestinal epithelium proliferation. However, injection of recombinant IL-11 or IL-22 does not induce enterocyte proliferation or a decrease in WGA$^+$ GCs in uninfected mice (Fig. 4, E and F), indicating that STAT3 activation is necessary, but not sufficient, to induce epithelial proliferation and requires another pathway which is induced by *Lm* infection.

(D) Confocal imaging of sections of the ileum obtained 4 d pi with 5 × 10^9 *Lm* and control. Tissue was fixed in Carnoy. Sections are stained for mucus (WGA), Muc2 mucin (Muc2), and nuclei (Hoechst). WGA$^+$ Muc2$^-$ cells located in the crypts are Paneth cells, which are not counted. Bars, 20 µm. **(E)** Quantification of WGA$^+$ GCs/villous in STAT3$^{IEC\text{-}WT}$ and STAT3$^{IEC\text{-}KO}$ mice infected by 5 × 10^9 *Lm* 4 d pi and noninfected control. *n* = 53–95 villi. Data are pooled from two independent experiments. Data are represented as mean ± SEM. Mann-Whitney test. **(F)** Quantification of Muc2$^+$ GCs/villous in STAT3$^{IEC\text{-}WT}$ and STAT3$^{IEC\text{-}KO}$ mice infected by 5 × 10^9 *Lm* 4 d pi and noninfected control. *n* = 53–95 villi. Data are pooled from two independent experiments. Data are represented as mean ± SEM. Mann-Whitney test. **(G)** Three-dimensional reconstruction of nonpermeabilized intestinal villi stained with WGA and for accessible Ecad and nuclei. **(H)** Quantification of WGA$^+$ GCs expressing or not accessible Ecad in STAT3$^{IEC\text{-}WT}$ and STAT3$^{IEC\text{-}KO}$ mice 4 d after inoculation of 5 × 10^9 *Lm* Δ*inlA* from the upper 100 µm of whole mount staining. *n* = 17–23 villi. Data are representative of two independent experiments with at least three mice per group. Data are represented as mean ± SEM. Mann-Whitney test. **(I)** *Lm* burden in intestine of STAT3$^{IEC\text{-}WT}$ and STAT3$^{IEC\text{-}KO}$ mice infected by WT *Lm* or the isogenic mutant Δ*inlA*. A first 3-d inoculation of 5 × 10^8 CFUs/animal was followed by a 4-d inoculation of 5 × 10^9 CFUs/animal. Data are pooled of five independent experiments. 13 mice per group for KIE16P mice infected by WT *Lm*; 10 mice per group for KIE16P mice infected by *Lm* Δ*inlA* and four mice per group for C57BL/6 infected by WT *Lm*. Wilcoxon test; animals are paired by subgroups for each experiment. *, P < 0.1; **, P < 0.01; ***, P < 0.001.

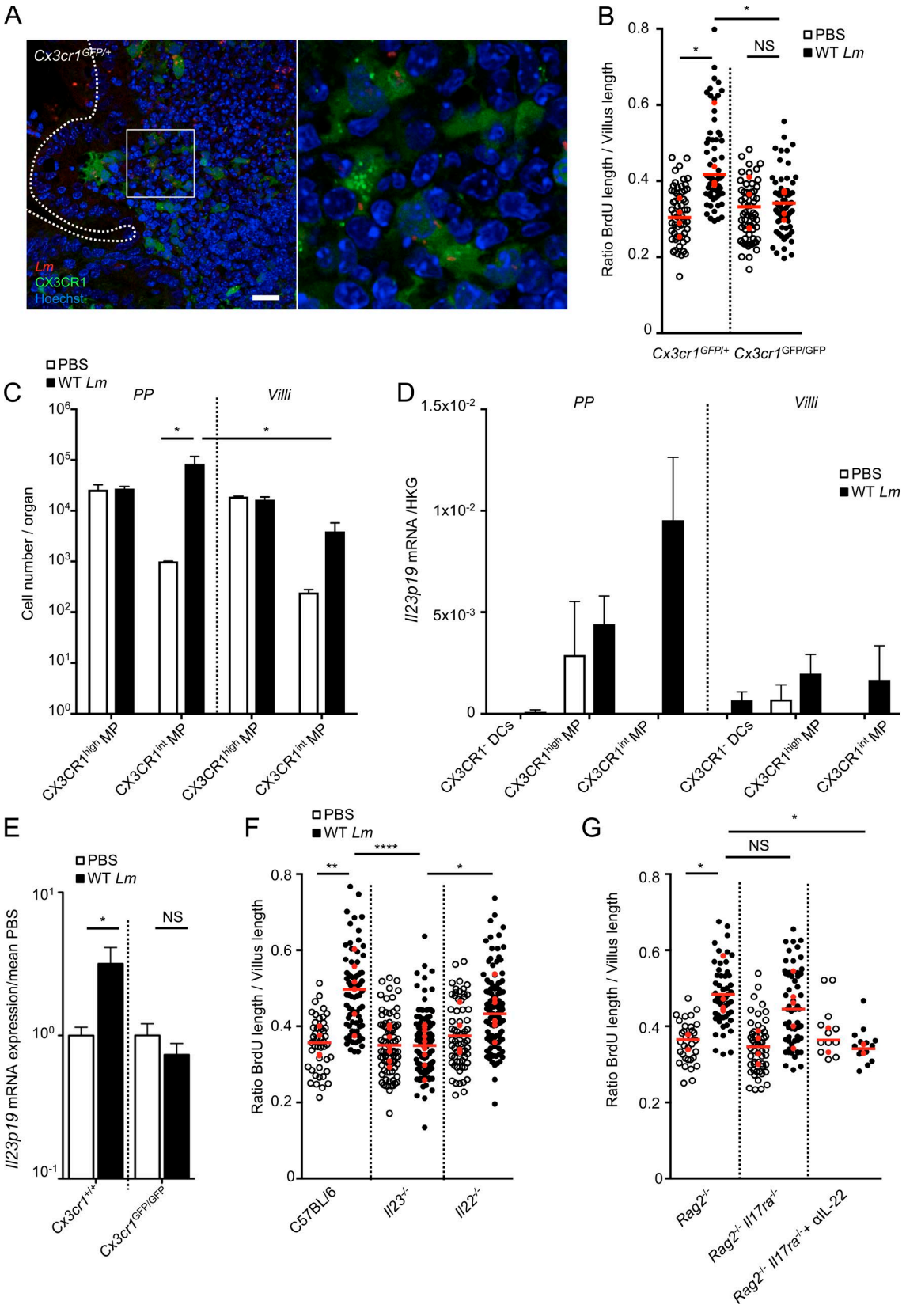

Figure 3. **IL-23 produced by CX3CR1 is involved in *Lm*-associated epithelial proliferation. (A)** Confocal imaging of a vibratome section from a PP infected by 5 × 10^9 *Lm* 24 h after oral inoculation. Bars, 20 µm. **(B)** Quantification of epithelial proliferation in *Cx3cr1*$^{GFP/GFP}$ and *Cx3cr1*$^{GFP/+}$ cohoused control mice 4 d after oral inoculation. **, P < 0.01; ***, P < 0.001. Each dot corresponds to one quantified villus, except the red dots, which correspond to the mean of each mouse. *n* = 4 mice/condition. Data are pooled from three independent experiments. A one-way ANOVA test followed by a Sidak's multiple comparisons was performed on the mean of each mouse. **(C)** Cell number per organ counted by flow cytometry. All PP versus entire intestinal tissue. Data are representative of

IFN-γ production by natural killer (NK) cells is required for *Lm*-associated epithelial response

IFN-γ is a major cytokine controlling *Lm* infection in vivo (Harty and Bevan, 1995). IFN-γ is also involved in tissue homeostasis, in particular in the intestine and liver (Smith et al., 2000; Brooling et al., 2005). We investigated enterocyte proliferation in *Ifnγ*$^{-/-}$ mice orally inoculated with *Lm*. As expected, IFN-γ depletion led to an increased *Lm* systemic burden (Fig. S4 A), yet no enterocyte proliferation was detectable, demonstrating the critical role of IFN-γ in *Lm*-associated enterocyte proliferation (Fig. 5 A). As previously shown, IFN-γ was mostly produced by NK cells and to a lower degree by T cells (Fig. 5 B and Fig. S4 B; Andersson et al., 1998; Reynders et al., 2011). *Lm*-associated enterocyte proliferation was still observed in *Rag2*$^{-/-}$ mice, which lack T and B cells, but was fully abolished in *Rag2*$^{-/-}$*γC*$^{-/-}$ mice, which also lack ILCs and NK cells (Fig. 5 C). To investigate if group 1 ILCs (including ILC1 and NK cells) are the cells involved in *Lm*-associated enterocyte proliferation, we depleted all ILC1 cells in *Rag2*$^{-/-}$*Il15*$^{-/-}$ mice injected with an antibody against NK1.1, a condition where ILC2s and ILC3s are preserved, but ILC1s are totally absent. *Lm*-associated epithelial proliferation was completely abrogated, as in *Rag2*$^{-/-}$*γC*$^{-/-}$ mice, indicating the essential role of ILC1s in *Lm*-associated enterocyte proliferation (Fig. 5 C).

We next investigated the signal triggering IFN-γ production by NK cells in response to *Lm* oral infection. It has been shown that CX3CR1^{+} cells produce IL-12 during sepsis (Ishida et al., 2008), leading to IFN-γ production by NK cells. Accordingly, CX3CR1^{+} MPs in PPs, but not in villi, expressed IL-12 in response to *Lm* infection (Fig. 5 D), and expression of both IFN-γ and IL-12 was CX3CR1-dependent (Fig. S4, C and D). IL-23 is a potent inducer of IFN-γ in *Helicobacter hepaticus* infection in mice (Buonocore et al., 2010). However, in our model, IFN-γ was induced after *Lm* infection in both WT and *Il23p19*$^{-/-}$ mice, indicating that in this context, IFN-γ production is IL-23 independent (Fig. S4 E).

IFN-γ can act both on hematopoietic and nonhematopoietic cells. To decipher if myeloid hematopoietic (radio-sensitive) or nonmyeloid nonhematopoietic (radio-resistant) cells are involved in IFN-γ–dependent *Lm*-associated enterocyte proliferation, we analyzed bone marrow chimera mice for which donor and recipient were either WT (C57BL/6) or *Ifnγr*$^{-/-}$ mice. C57BL/6→*Ifnγr*$^{-/-}$ and *Ifnγr*$^{-/-}$→C57BL/6 mice chimeras were generated and infected with *Lm*. Proliferation was impaired when IFN-γR$^{-/-}$ cells were radio-resistant, but not radio-sensitive, indicating a role of nonhematopoietic cells, likely epithelial cells, in IFN-γ–dependent proliferation (Fig. 5 E).

STAT3 and STAT1 activations lead to intestinal enterocyte proliferation

Both IL-22 and IL-11, known to activate STAT3 and IFN-γ, which activates STAT1, are required in vivo for *Lm*-associated enterocyte proliferation. IL-22/IL-11 and IFN-γ are expressed 24–48 h pi (data not shown; Reynders et al., 2011). To determine whether IL-22, IL-11, and IFN-γ act in an interdependent and direct manner on epithelial cells to induce proliferation, we used intestinal organoids. We first determined by Western blotting that STAT3 is phosphorylated upon IL-22 or IL-11, but not IL-23, treatment of intestinal organoids and that STAT1 is phosphorylated upon IFN-γ treatment, indicating a direct effect of these cytokines on epithelial cells (Fig. S4, F and G). As expected, induction of proliferation in organoids did not occur with IL-23 (data not shown). It also did not occur with IL-22 or IFN-γ alone, indicating that these cytokines are not sufficient to induce proliferation (Fig. 6 A and Fig. S4 I for the method). In contrast, proliferation was observed when both a STAT3 inducer (IL-22 or IL-11) and a STAT1 inducer (IFN-γ) were simultaneously added to intestinal organoids (Fig. 6, A–C). STAT3 excision by the addition of hydroxytamoxifen to *Stat3*$^{fl/fl}$ *Villin-cre* intestinal organoids blocked proliferation induced by IL-22 and IFN-γ, indicating the critical requirement for STAT3 in proliferation (Fig. 6 D and Fig. S4 H). STAT1 inhibitor fludarabine (Frank et al., 1999) also led to a decrease in proliferation, indicating that both STAT3 and STAT1 activators are required to induce epithelial cell proliferation (Fig. 6 E).

Lm infection increases susceptibility to colitis

We have previously shown that *Lm* also targets the cecum and colon (Disson et al., 2008). We investigated if *Lm* regulates epithelial homeostasis at the cecum and colon level. We observed an increase of proliferation in the colon (Fig. S5 A), as well as a decrease in the number of WGA^{+} GCs upon *Lm* infection, while the number of Muc2^{+} GCs was not modified (Fig. S5, B and C). Depletion of mucus sensitizes mice to colitis (Van der Sluis et al., 2006). We therefore investigated the impact of *Lm*-associated WGA^{+} GC depletion on luminal mucus content and its consequences on susceptibility to colitis. The distance between the microflora and the epithelium, which reflects mucus thickness, was strongly decreased in a STAT3-dependent manner in the ileum and cecum (Fig. S5, D–G). At the colon level, the thickness of the highly organized inner mucus layer, measured by a Muc2^{+} staining, was reduced upon *Lm* infection (Fig. 7, A and B). Thus, *Lm*-associated decrease of the differentiation of the GCs inhibits *Lm* entry, while leading to a significant decrease in the physical

two independent experiments with three mice per group. Data are represented as mean ± SEM. A one-way ANOVA test followed by a Sidak's multiple comparisons was performed on the mean of each mouse. **(D)** *Il23p19* mRNA quantification by qRT-PCR on sorted PPs and villi CX3CR1^{-} and CX3CR1^{+} cells 24 h pi. Data are representative of two independent experiments with at least three mice per group. Data are represented as mean ± SEM. **(E)** *Il23p19* mRNA quantification by qRT-PCR from intestinal tissue of *Cx3cr1*$^{GFP/GFP}$ and *Cx3cr1*$^{GFP/+}$ mice 24 h pi. Data are pooled of three independent experiments. Six *Cx3cr1*$^{+/+}$ mice; seven *Cx3cr1*$^{GFP/GFP}$ mice. Data are represented as mean ± SEM. Student's *t* test. **(F)** Quantification of epithelial proliferation in control cohoused C57BL/6 and mutant mice 4 d after oral inoculation. Each dot corresponds to one quantified villus, except the red dots, which correspond to the mean of each mouse. *n* = 4–9 mice/condition. Data are pooled from four independent experiments. A one-way ANOVA test followed by a Sidak's multiple comparisons was performed on the mean of each mouse. **(G)** Quantification of epithelial proliferation in cohoused *Rag2*$^{-/-}$ and *Rag2*$^{-/-}$*IL17ra*$^{-/-}$ injected or not with a blocking αIL-22 antibody 4 d after oral inoculation. Each dot corresponds to one quantified villus, except the red dots, which correspond to the mean of each mouse. *n* = 12–57 villi. Data are pooled of two independent experiments. A one-way ANOVA test followed by a Sidak's multiple comparisons was performed on the mean of each mouse. *, P < 0.05; **, P < 0.01; ****, P < 0.0001.

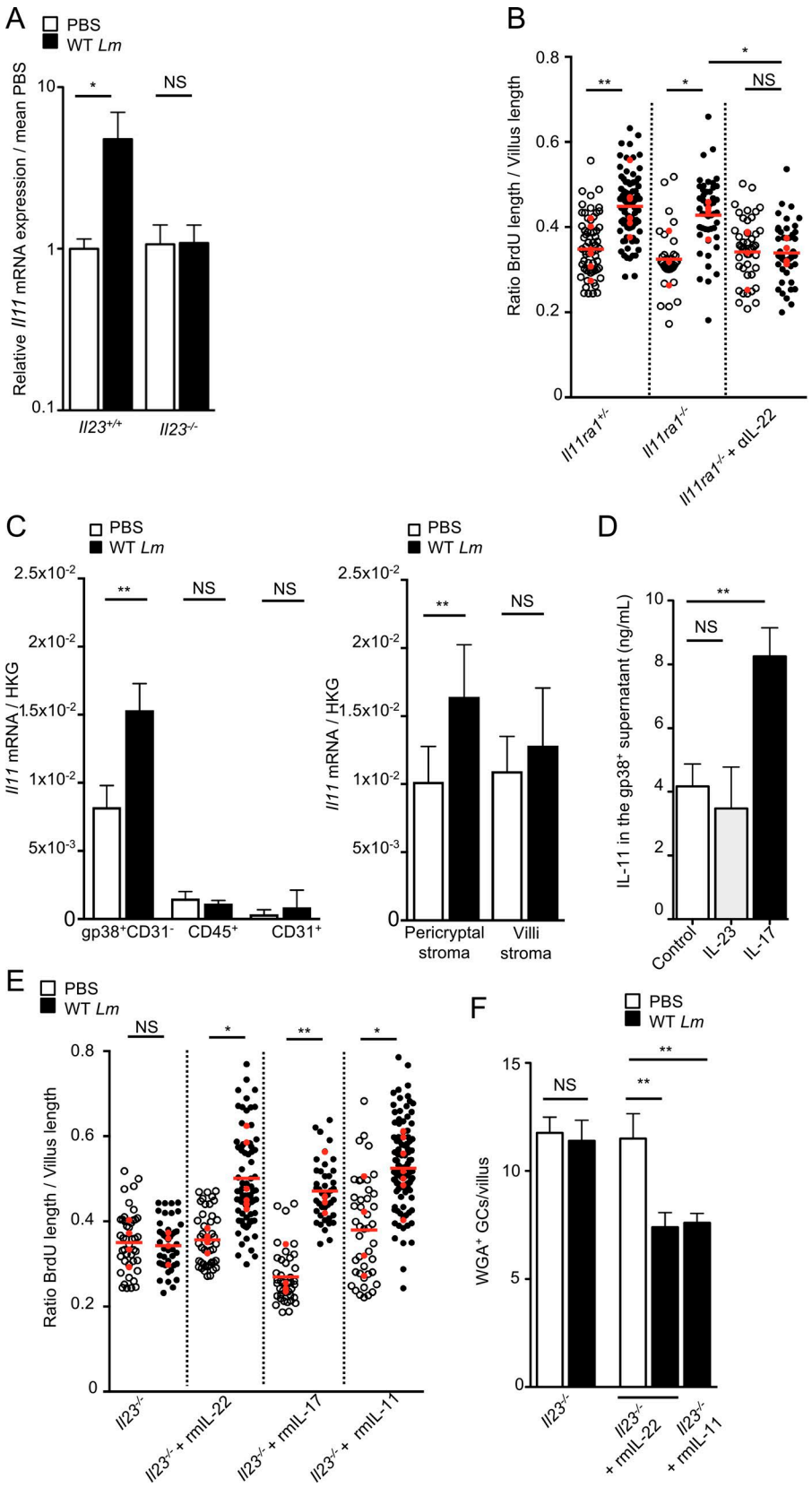

Figure 4. **IL-11 expressed by Gp38⁺ stromal cells in an IL-23–dependent manner is involved in *Lm*-associated epithelial proliferation. (A)** *Il11* mRNA quantification by qRT-PCR from intestinal tissue of *Il23*$^{+/+}$ and *Il23*$^{-/-}$ mice 48 h pi. Data are pooled of two independent experiments. Five *Il23*$^{+/+}$ mice; four *Il23*$^{-/-}$ mice. Data are represented as mean ± SEM. Student's *t* test. **(B)** Quantification of epithelial proliferation in littermate *Il11ra1*$^{+/-}$ and *Il11ra1*$^{-/-}$ mice injected or not with a blocking αIL-22 antibody 4 d after oral inoculation. Each dot corresponds to one quantified villus, except the red dots, which correspond to the mean of each mouse. At least 5 fields/10 villi per mouse. *n* = 3–8 mice/condition. Data are pooled of three independent experiments. A one-way ANOVA test followed by a Sidak's multiple comparisons was performed on the mean of each mouse. **(C)** *Il11* mRNA quantification by qRT-PCR from sorted LP populations, as indicated, 48 h pi. Data are representative of two independent experiments. Three animals per group. Data are represented as mean ± SEM. Student's *t* test. **(D)** IL-11 protein quantification by an ELISA assay from sorted CD45^{-} gp38^{+} stromal cells stimulated in vitro with the indicated cytokines. Data are pooled of three independent experiments. Six culture wells per condition. Data are represented as mean ± SEM. Mann-Whitney test. **(E)** Quantification of epithelial proliferation in *Il23*$^{-/-}$ littermate mice complemented with rmIL-22, rmIL-17, and rmIL-11 4 d after oral inoculation. Each dot corresponds to one quantified villus except the red dots, which correspond to the mean of each mouse. *n* = 4–7 mice/condition. Data are pooled of three independent experiments. A one-way ANOVA test followed by a Sidak's multiple comparisons was performed on the mean of each mouse. **(F)** Quantification of WGA^{+} GCs/villous in *Il23*$^{-/-}$ mice complemented with recombinant IL-11 and IL-22, infected by 5 × 10^{9} *Lm* 4 d pi and noninfected control. *n* = 10–30 villi. Data are representative of two independent experiments. Data are represented as mean ± SEM. Mann-Whitney test. *, P < 0.05; **, P < 0.01.

separation between the epithelium and the luminal content, a well-established risk factor for colitis. To investigate whether *Lm*-associated decrease in mucus layer increases susceptibility to colitis, we fed mice with DSS for seven consecutive days, 7 d after *Lm* Δ*inlA* infection, when the IL-23 and IFN-γ pathways are no more induced (our observation; Reynders et al., 2011). Mice were sacrificed 14 d pi, and the colitis was evaluated. Infection with *Lm* Δ*inlA* alone, which does not invade epithelial cells, did not

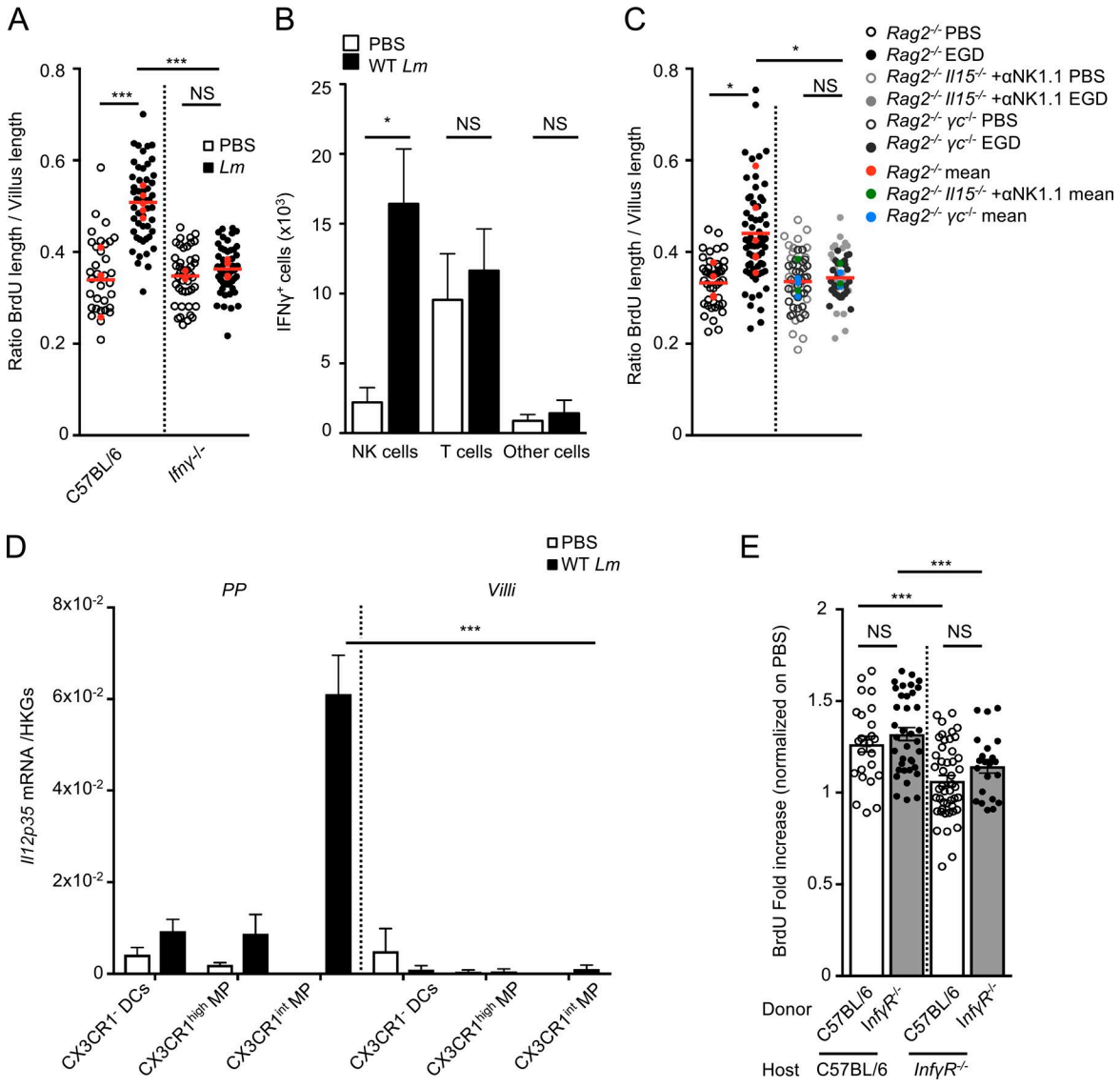

Figure 5. **IFN-γ produced by NK cells is involved in *Lm*-associated epithelial proliferation. (A)** Quantification of epithelial proliferation in cohoused C57BL/6 control and *Ifnγ*$^{-/-}$ mice 4 d after oral inoculation. Each dot corresponds to one quantified villus, except the red dots, which correspond to the mean of each mouse. At least 5 fields/10 villi per mouse. *n* = 3–5 mice/condition. Data are pooled of two independent experiments. A one-way ANOVA test followed by a Sidak's multiple comparisons was performed on the mean of each mouse. **(B)** Quantification by flow cytometry analysis of IFN-γ^{+} cells. Data are pooled of three independent experiments. *n* = 4–5 animals per group. Data are represented as mean ± SEM. Student's *t* test. **(C)** Quantification of epithelial proliferation in cohoused *Rag2*$^{-/-}$, *Rag2*$^{-/-}$ γc$^{-/-}$, *Rag2*$^{-/-}$*Il15*$^{-/-}$ injected with a blocking αNK1.1 antibody 4 d after oral inoculation. Each dot corresponds to one quantified villus, except the red, green, and blue dots which correspond to the mean of each mouse. *n* = 3–6 mice per condition. Data are pooled of two independent experiments. A one-way ANOVA test followed by a Sidak's multiple comparisons was performed on the mean of each mouse. **(D)** *Il12p35* mRNA quantification by qRT-PCR on sorted PPs and villi CX3CR1^{-} and CX3CR1^{+} cells 24 h pi. Data are representative of two independent experiments with at least three mice per group. Data are represented as mean ± SEM. Student's *t* test. **(E)** Quantification of epithelial proliferation in C57BL/6:*IfnγR*$^{-/-}$ and *IfnγR*$^{-/-}$:C57BL/6 chimera mice 4 d after oral inoculation. Data are pooled of two independent experiments with two to four mice per group. *, P < 0.05; **, P < 0.01; ***, P < 0.001.

induce gut lesions 14 d pi, and pathology was similar to noninfected control (Fig. 7 C, top and second from bottom; and Fig. 7 D). As previously described, DSS treatment of noninfected mice induced colitis (Okayasu et al., 1990), as quantified by colonic inflammation and epithelial and mesenchymal lesions (Fig. 7 C, second from top; and Fig. 7 D). Very interestingly, as compared with controls treated by DSS only or with an *Lm* Δ*hly* strain (Fig. S5 H), with which *Lm*-associated intestinal response is abolished, animals exposed to *Lm* Δ*inlA* before DSS, in which the mucus thickness was reduced, developed significantly more severe colitis (Fig. 7 C, bottom; and Fig. 7 D). Altogether, this indicates that *Lm* significantly increases susceptibility to colitis.

Discussion

In contrast to other foodborne infections, the intestinal phase of listeriosis is clinically silent in most patients (Charlier et al., 2017). In line with this observation, the crossing of the intestinal barrier by *Lm* is not associated with epithelial damage, in contrast to other enteropathogens such as *S. enterica*, *S. flexnerii*,

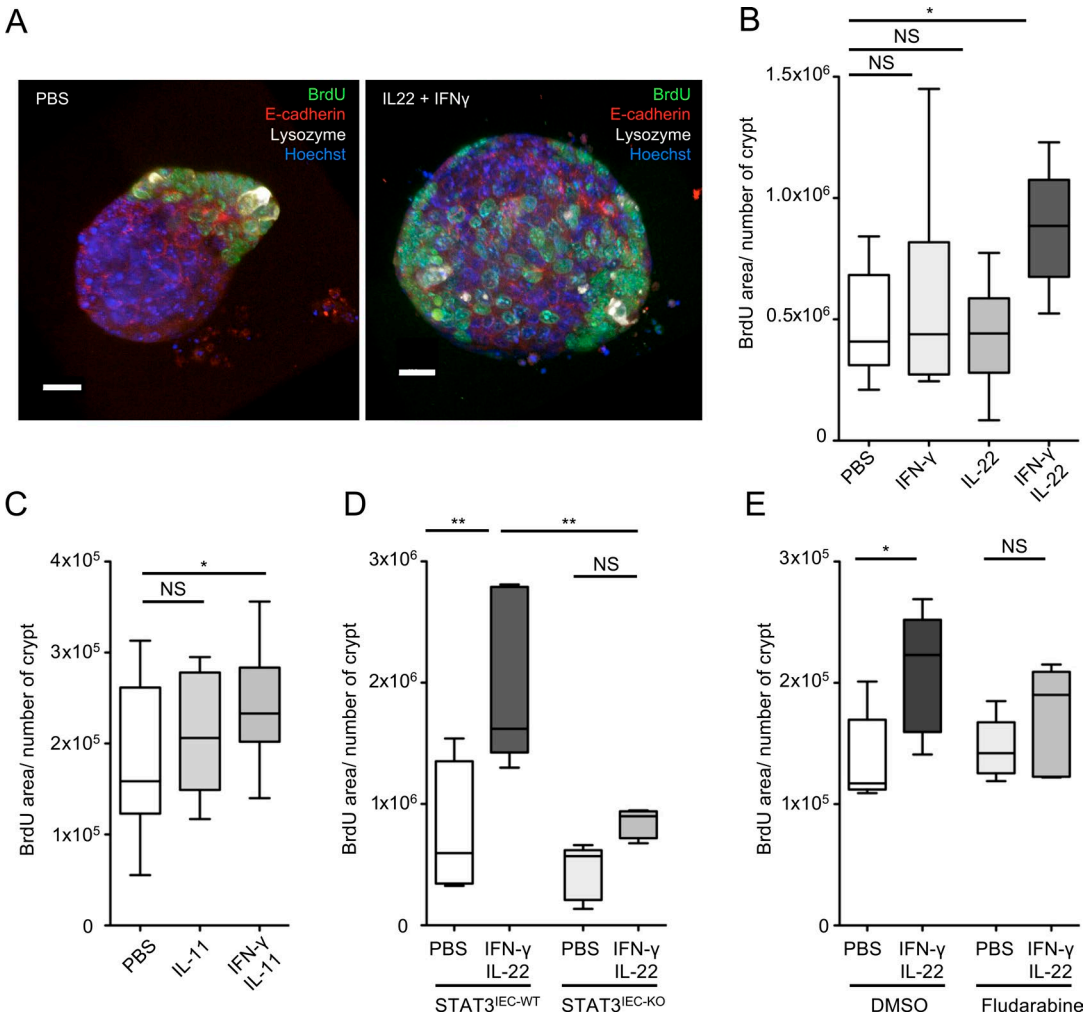

Figure 6. **IL-23 and IFN-γ pathways complement to induce epithelial proliferation. (A)** Maximum intensity projection of Z stacks from organoids incubated with the indicated cytokines. **(B)** Quantification of BrdU incorporation in organoids incubated with the indicated cytokines and treatment, detailed in the supplemental procedures. *n* = 8–10 pooled organoids from two independent experiments. A one-way ANOVA test followed by a Sidak's multiple comparisons was performed. **(C)** Quantification of BrdU incorporation in organoids incubated with the indicated cytokines and treatment, detailed in the supplemental material. *n* = 15–17 pooled organoids from three independent experiments. A one-way ANOVA test followed by a Sidak's multiple comparisons was performed. **(D)** Quantification of BrdU incorporation in organoids incubated with the indicated cytokines and treatment, detailed in the supplemental material. *n* = 4 (PBS) or 5 (IFN-γ + IL-22) organoids pooled from two plates, representative of two independent experiments. A one-way ANOVA test followed by a Sidak's multiple comparisons was performed. **(E)** Quantification of BrdU incorporation in organoids incubated with the indicated cytokines and treatment, detailed in the supplemental material. *n* = 5 organoids pooled from two plates for each condition. A one-way ANOVA test followed by a Sidak's multiple comparisons was performed. *, P < 0.05; **, P < 0.01.

and *C. rodentium*, a model for attaching/effacing pathogens in mice inducing epithelial lesions (Collins et al., 2014). Here, we have shown that upon *Lm* infection, PP CX3CR1$^+$ cells trigger both IL-23/IL-22/IL-11 and IFN-γ pathways, which act in combination to accelerate epithelial cell renewal and decrease the number of WGA$^+$ GCs expressing accessible Ecad. This leads to a complete blockade of intestinal villus invasion by *Lm*. Unexpectedly, this response, which critically requires IL-23, is partially IL-22–dependent and requires the expression of IL-11 by intestinal gp38$^+$ stromal cells (Fig. 8).

The number of GCs and their differentiation are modulated upon infection with other enteropathogens. Indeed, *C. rodentium* leads to a depletion of GCs and a decrease in the thickness of the mucus layer during the first phase of the infection, which is reversed during the clearance of the infection (Gustafsson et al., 2013). *C. rodentium* and *Salmonella typhimurium* modulate GC number in an IFN-γ–dependent manner, and IFN-γ is expressed by CD4 T$^+$ cells in the case of *C. rodentium* infection (Songhet et al., 2011; Chan et al., 2013; Klose et al., 2013). *Lm* translocation across intestinal epithelium at the villus level occurs in an InlA-dependent manner via luminally accessible Ecad on GCs (Nikitas et al., 2011). Decrease of WGA$^+$ GC number expressing luminally accessible Ecad in response to *Lm* therefore selectively blocks InlA-dependent translocation of *Lm* at the villus level and constitutes a novel and specific innate immune mechanism against an enteropathogen (Fig. S1 A and Fig. 8).

This pathway, which is not initiated upon villus infection, is triggered at the PP level. This is in agreement with previously published results showing that host response to *Lm* at the intestinal level is fully dependent on *Lm* PP infection (Lecuit et al.,

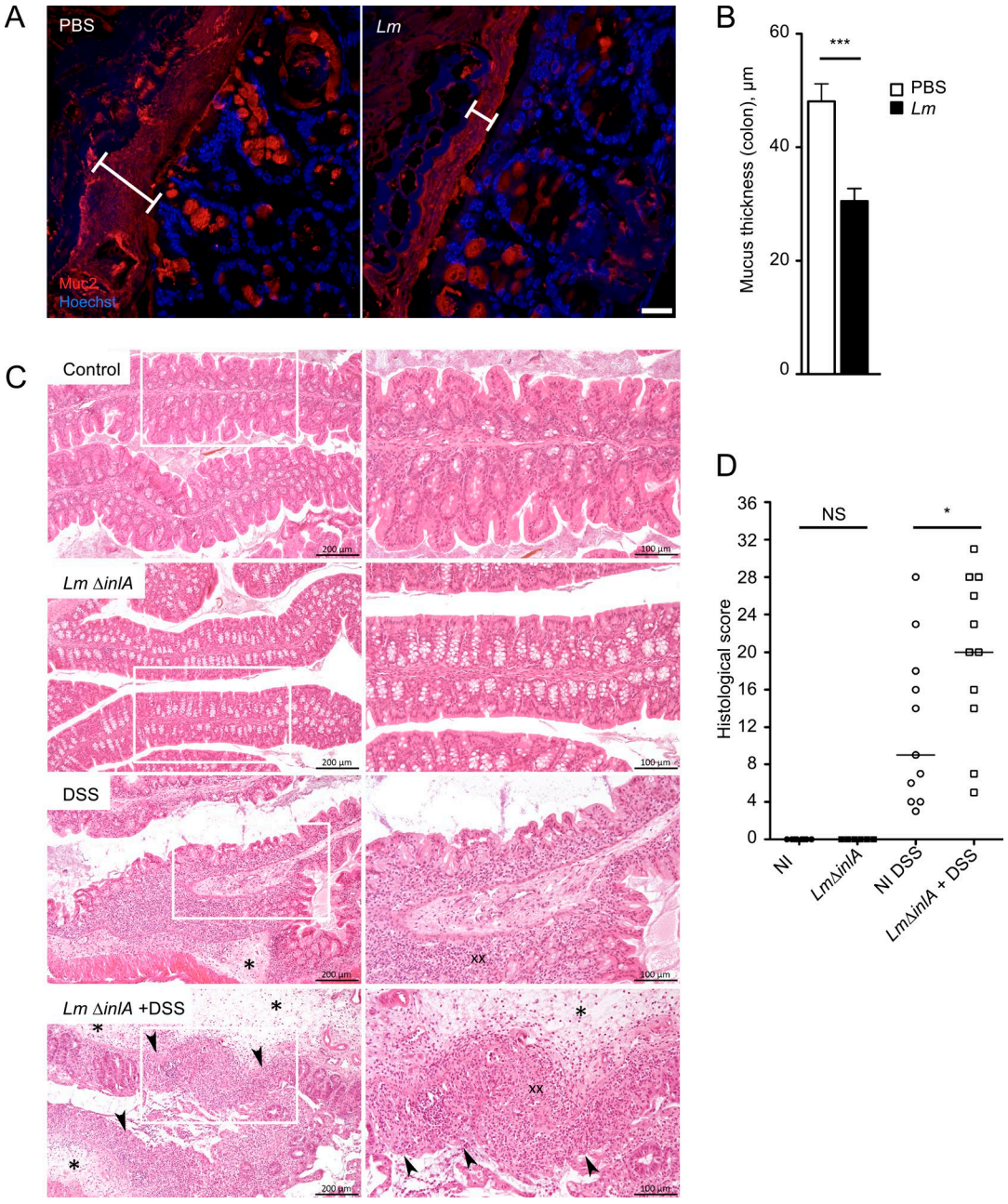

Figure 7. ***Lm*-associated sensitization to colitis. (A)** Confocal imaging of sections of Carnoy's fixed colons 4 d pi, 5 × 10^9 *Lm ΔinlA*. Sections are stained for Muc2 mucin (Muc2) and nuclei (Hoechst). Bars, 20 µm. **(B)** Quantification of mucus thickness, in µm. *n* = 26 to 31 measures. Data are represented as mean ± SEM. Mann-Whitney test. **(C)** Hematoxylin and eosin staining of *Lm ΔinlA*-infected and DSS-treated mice. **(D)** Score of histological lesions induced in DSS-treated mice. One point represents one mouse. NI, not infected; DSS, DSS-treated mice. Data are pooled from two independent experiments. A one-way ANOVA test followed by a Sidak's multiple comparisons was performed. *, P < 0.05; ***, P < 0.001.

2007). Our results further illustrate that invasion of villi via GCs in an InlA-dependent manner is silent. This study underlines on one hand the relative unresponsiveness of the villus LP to pro-inflammatory stimuli and on the other hand the critical role of PP in danger detection and propagation of defense signals to the intestinal epithelium.

IL-22 induces epithelial proliferation through STAT3 activation during DSS-induced colitis (Pickert et al., 2009) and is expressed downstream of IL-23 in response to *C. rodentium* infection in the colon (Aychek et al., 2015). However, although epithelial proliferation is fully IL-23 and STAT3 dependent upon *Lm* infection, IL-22 only partially relays IL-23 signaling at the intestinal level. We have shown here that IL-17, which is produced by γδ T cells upon *Lm* infection (Hamada et al., 2008; Sheridan et al., 2013), induces *Lm*-associated enterocyte proliferation together with IL-22. IL-17 in turn triggers IL-11 expression by LP gp38$^+$CD34$^+$ stromal cells, which activates STAT3 in epithelial cells (Fig. 8). IL-11 is a known activator of STAT3, involved in gastrointestinal tumorigenesis in human and in mouse (Putoczki et al., 2013). IL-11 is also induced upon *C. rodentium*, by a so-far unknown

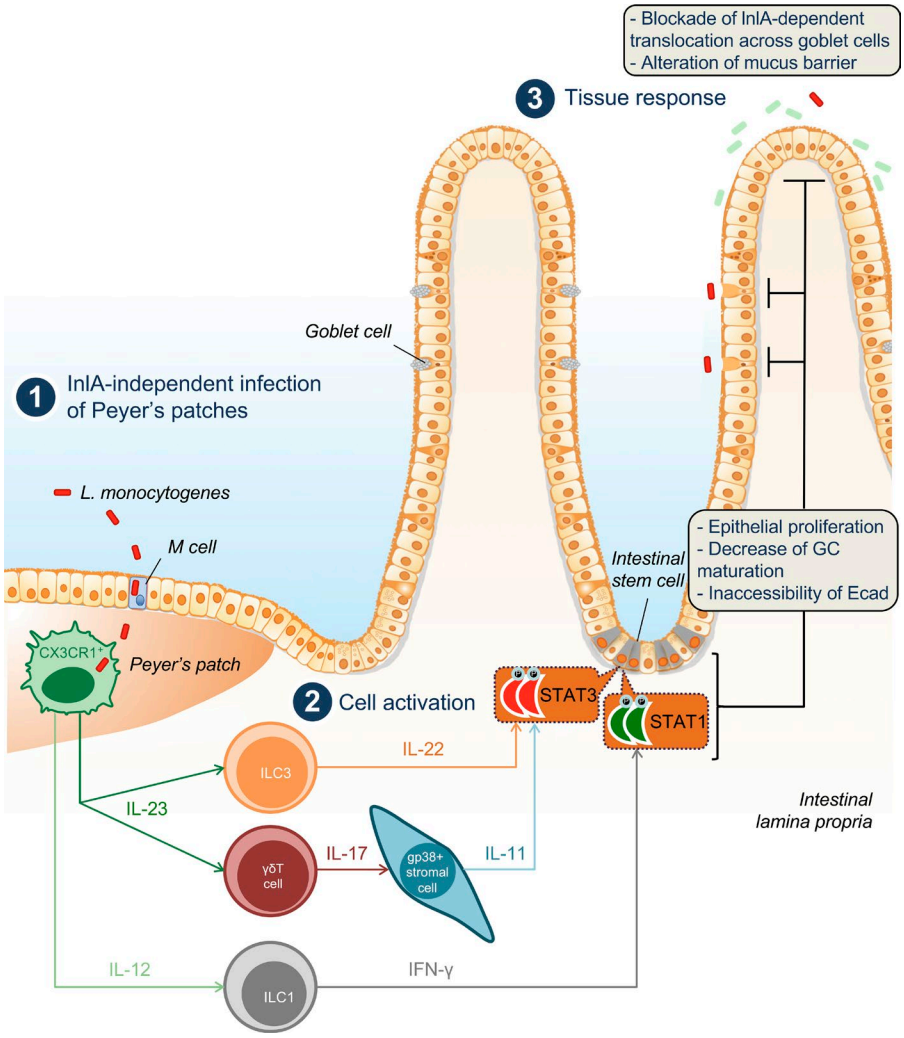

Figure 8. **Model of the mechanisms and downstream effects induced by *Lm* infection at the villus epithelial level.** *Lm* infects CX3CR1$^+$ cells in PPs (in an InlA-independent manner; 1), triggering both IL-23–IL-22–IL-11 and IL-12–IFN-γ pathways (2). Activation of STAT3 and STAT1 in intestinal epithelial cells leads to an increase of epithelial proliferation and a decrease of goblet cells expressing accessible Ecad. As a consequence, *Lm* intestinal villus invasion via GCs (which is InlA/Ecad dependent) is blocked, and mucus barrier is altered (3).

mechanism and is involved in protection against TLR4-mediated colitis (Gibson et al., 2010). Whereas inhibition of IL-11 does not exacerbate *Lm* burden in systemic listeriosis (Opal et al., 2000), the role of IL-11 during *Lm* oral infection had so far not been investigated. Several cell types have been described to express IL-11 in the intestine (Putoczki and Ernst, 2010). We show here that LP gp38$^+$CD34$^+$ stromal cells, a mesenchymal cell subset in close contact with the intestinal crypts, are the major intestinal source of IL-11 upon *Lm* infection. Several evidences indicate that mesenchymal stromal cells are involved in mucosal immune responses, notably via IL-33 (Owens and Simmons, 2013; Mahapatro et al., 2016). Here, we have uncovered that gp38$^+$CD34$^+$ stromal cells are part of a host response pathway involving CX3CR1-derived IL-23 and γδ T–derived IL-17, which leads to intestinal epithelial cells proliferation and depletion of GCs expressing accessible Ecad in a STAT3-dependent manner in response to an enteric infection. The partially redundant and complementary roles of IL-11 and IL-22 upon *Lm* infection remain to be characterized in more detail. We have shown that IL-11 effect is compensated by IL-22 in *Il11ra*$^{-/-}$ mice, but is unmasked when IL-22 is also absent. The induction of STAT3 via the respective receptors of IL-11 and IL-22 may allow the fine tuning in time and space of host tissue responses to infection (Ernst et al., 2014).

IL-22 and IL-11 are not sufficient to induce proliferation and GC depletion in noninfected mice, indicating that a cofactor induced by *Lm* infection is necessary. IFN-γ is expressed upon *Lm* infection (Andersson et al., 1998), and both IL-22 and IFN-γ are induced in an InlA-independent manner 24 h pi and peak 48 h pi upon *Lm* oral infection (Reynders et al., 2011), indicating that they may act together rather than sequentially. We could recapitulate ex vivo stem cells proliferation by simultaneously treating with IL-22 and IFN-γ intestinal organoids. These results indicate that IL-22/IL-11–dependent STAT3 phosphorylation is not sufficient to induce proliferation, which indeed requires STAT1 phosphorylation, in response to IFN-γ receptor engagement. In line with this finding, IL-22–dependent STAT3-induced proliferation is involved in vivo in tissue repair in a graft-versus-host tissue damage model (Lindemans et al., 2015) and DSS-induced colitis (Pickert et al., 2009; Geng et al., 2018). IL-22 and IFN-γ are also induced upon the protozoan *Tritrichomonas musculis* infection, which increases susceptibility to colorectal cancer induced in *Apc*$^{min/+}$ mice (Chudnovskiy et al., 2016).

WGA$^+$ GC depletion and the decrease of luminally accessible Ecad constitute a specific and very efficient short-term host defense response to *Lm* infection, by locking its portal of entry (Fig. 8 and Fig. S5 I). But this response is also potentially detri-

mental for the host by reducing the thickness of the protective mucosal barrier all along the gut and especially in the colon where the mucus layer is highly organized. Decrease of mucus layer thickness has been shown to be associated with the development of colitis (Van der Sluis et al., 2006). In line with these results, we show here that *Lm* increases host susceptibility to colitis. This provides support to previous report on the association between *Lm* presence in the gut and the development of inflammatory bowel disease (IBD; Liu et al., 1995; Hugot et al., 2003; Miranda-Bautista et al., 2014). Decrease of mucus layer thickness has also been shown to be associated with colorectal cancer (Velcich et al., 2002) and Crohn's disease (Niv, 2016). IL-23, IL-22, and IL-11 can promote tumor growth in a mouse model of colorectal tumorigenesis (Grivennikov et al., 2012; Putoczki et al., 2013) and are associated with IBD (Eken et al., 2014). Chronic *Lm* intestinal carriage is more likely in Western countries where refrigeration favors *Lm* food contamination and human exposure (Swaminathan and Gerner-Smidt, 2007) and may be associated with gallbladder infection (Begley et al., 2009; Charlier et al., 2014). This study suggests that chronic *Lm* intestinal carriage may favor both IBD and tumorigenesis, through both decreased mucus layer thickness and production of cytokines such as IL-23 and IL-11, in conjunction with host factor predisposing for these conditions. This hypothesis is in line with the highest incidence of IBD and colon cancer in Western countries (Ng et al., 2013; Kuipers et al., 2015). Assessing the biological and medical relevance of this correlation will require further epidemiological and experimental studies.

Materials and methods

Mice and infection

All the procedures were in agreement with the guidelines of the European Commission for the handling of laboratory animals, directive 86/609/EEC. They were approved by the ethical committees No. 59 under the number 2010-0020 and by the CET EA/CEEA No. 89 under the numbers HA0017, 2015-0014, and 2017-0057. Knock-in E16P mouse line was from our laboratory. *Cx3cr1*^{GFP} mice (Jung et al., 2000; RRID: MGI:2670353) were provided by the Cryopréservation, Distribution, Typage et Archivage Animal Orléans, Orléans, France. *Il23p19*$^{-/-}$ mice (Ghilardi et al., 2004) were provided by Genentech through B. Ryffel (CDTA Orléans). *Rag2*$^{-/-}$, *Rag2*$^{-/-}\gamma c^{-/-}$, *Rag2*$^{-/-}$*Il17ra*$^{-/-}$, and *Rag2*$^{-/-}$ *Il15*$^{-/-}$ were provided by the laboratory of J. Di Santo. *Il22*$^{-/-}$ mice were provided by R. Flavell (Yale University School of Medicine, New Haven, CT) via C. Leclerc (Institut Pasteur, Paris, France; Zenewicz et al., 2007). *Il11ra*$^{-/-}$ mice were provided by T. Putoczki (University of Melbourne, Parkville, Australia; Nandurkar et al., 1997). *Stat3*$^{fl/fl}$ *Villin-cre* mice are from *Stat3*$^{fl/fl}$ mice (Takeda et al., 1998) crossed with *Villin-Cre* (*Cre-Ert2*) mice (El Marjou et al., 2004). C57BL/6J were provided by Janvier Laboratories. 6–12-wk-old animals were used.

Littermates were used (KIE16P, STAT3^{IEC}, and KIE16P STAT3^{IEC} mice; *Il11ra*$^{+/-}$, *Il11ra*$^{-/-}$, *CX3CR1*$^{GFP/+}$, and *CX3CR1*$^{GFP/GFP}$ mice; as well as *Il23p19*$^{-/-}$ mice treated with rmIL-11, rmIL-22, rm-IL-17, and anti–IL-22 and *Rag*$^{-/-}$ *Il15*$^{-/-}$ mice treated with anti-NK1.1). When necessary, control C57BL/6J were housed in the same animal facility at least 2 wk before being handling for experiments to avoid a bias coming from microbiota differences and mixed with the other animals in the same cage if possible. In each experiment, control KIE16P or C57BL/6J were used to have an internal control. Germ-free mice were housed in dedicated isolators.

For infection, *Lm* (EGD, EGDe, and isogenic mutants) fresh colonies were diluted in brain–heart infusion medium to reach mid-log growth phase. For intragastric gavage, 200 µl of bacteria in PBS were mixed with 300 µl of $CaCO_3$ (50 mg/ml^{-1}) before injection in overnight starved animals. For BrdU assays, 150 µl of BrdU-labeling reagent solution (10373283; Life Technologies) were injected i.p. 16 h before sacrifice. To monitor bacterial burden, organs were removed from infected killed animals and homogenized. Before homogenization, intestines were rinsed twice with DMEM and incubated for 2 h at room temperature in DMEM supplemented with gentamicin (100 mg/ml; Sigma-Aldrich). Serial dilutions of cell suspensions in PBS were plated on brain–heart infusion agar plates. After 24 h of incubation at 37°C, CFUs were counted.

For in vivo IL-22 blocking experiments, mice were injected i.p. either with PBS (control) or with 0.3 mg purified anti–IL-22 (AM22.1 provided by J.C. Renauld and L. Dumoutier, Université Catholique de Louvain, Brussels, Belgium) at days −3 and 0 of infection. To deplete NK1.1$^+$ cells, control and *Lm*-infected *Rag2*$^{-/-}$ *il15*$^{-/-}$ mice were injected i.p. with 100 µg of anti-NK1.1 antibody (PK136; Biolegend) in 0.1 ml PBS 1 d before *Lm* injection.

For in vivo cytokine treatment, mice were injected with 5 ng/g of mouse recombinant IL-22 (R&D; 582-ML-CF) or mouse recombinant IL-11 (R&D; 418-ML-CF) or mouse recombinant IL-17 (R&D; 421-ML-CF) at day −1, 0, 1, 2, and 3 after injection.

Hydroxytamoxifen treatment

Hydroxytamoxifen was dissolved in corn oil at 10 mg/ml. *Stat3*$^{fl/fl}$ *Villin-cre* mice were treated for five consecutive days with 1 mg/d, as previously described (Indra et al., 1999), 7 d before infection.

Bone marrow engraftment

Total bone marrow cells were removed from legs (femora and tibiae) of donor WT mice and intravenously injected into 5-wk-old lethally irradiated (1,250 rad) host mice (one donor for four recipient mice) to generate bone marrow chimera. After 10–12 wk of bone marrow reconstitution, chimeras were used to perform experiments.

Biotin penetration experiment

Biotin was used as a molecule to address the integrity of intestinal epithelium as described previously (Tsai et al., 2013). In brief, 2 mg/ml of EZ-link Sulfo-NHS-Biotin (Pierce) in PBS was slowly injected into the lumen of ileum loop via the open end adjacent to cecum immediately after removal of the entire ileum. After 3 min, the loop was opened and followed by PBS wash and 4% paraformaldehyde (PFA) fixation.

Ligated loops

8–12-wk-old mice were fasted for 16 h before surgery. 30 min after injection of the buprenorphine (0.1 mg/kg body weight), deep anesthesia was induced with a mix of ketamine (100

mg/kg body weight; Imalgene 1000; Merial), and xylazine chlorhydrate (10 mg/kg body weight; Rompun; Bayer). Skin was cleaned with Vetadine, a laparotomy was performed, the small intestine was exposed, and ileal loops of 1.5-cm long containing or not containing one PP were prepared. 100 µl of inoculum (10^5 CFUs) was injected into each loop. Loop was placed back in the peritoneal cavity. PBS was injected subcutaneously to prevent dehydration and BrdU was injected intraperitoneally. Peritoneal membrane and skin were sutured, and animals were returned to their warmed cage. Water was allowed, but not food. 24 h pi, mice were killed. Intestinal loops were harvested, washed in PBS, and fixed in 4% PFA overnight. Tissue staining is described below.

Quantitative real-time PCR (qRT-PCR)

We performed RNA isolation and qRT-PCR as previously described (Dulauroy et al., 2012). In brief, we extracted total RNA from FACS-sorted cells using RNeasy Micro kit (Qiagen) and assessed the quality of total RNA using the 2100 Bioanalyzer system (Agilent Technologies). Transcription was performed using Superscript III reverse transcription (Invitrogen). All procedures were performed according to the manufacturers' protocols. We performed qRT-PCR using RT^2-qPCR primer sets (SABiosciences) and RT^2 SYBR-green master mix (SABiosciences) on a PTC-200 thermocycler equipped with a Chromo4 detector (Bio-Rad Laboratories) and analyzed data using Opticon Monitor software (Bio-Rad Laboratories). We normalized C_t values to the mean C_t values obtained for the housekeeping genes *Hsp90ab1*, *Hprt*, and *Gapdh*.

Cell isolation, flow cytometry analysis, and sorting

Isolation of intestinal myeloid and stromal cells were performed as previously described (Satoh-Takayama et al., 2008; Stzepourginski et al., 2015). Cells were blocked and stained with indicated antibodies: CD3 (clone 145-2C11; eBioscience); CD19 (clone 1D3; BD); NKp46 (clone 29A1.4; eBioscience); IFN-γ (clone XMG1.2; BD); NK1.1 (clone PK136; Biolegend); and CD31 (clone 390; eBioscience). Syrian hamster antibody to gp38 was a gift from A. Farr (University of Washington, Seattle, WA).

Cells were analyzed with an LSRFortessa flow cytometer (BD) or sorted with a FACSAria machine (BD). Flow cytometry analysis was done with the FlowJo software (Tree Star). Sorted stromal CD45$^-$gp38$^+$ cells were grown in DMEM containing 10% fetal calf serum at 150,000 cells/well in 24-well plates coated with rat tail collagen (10 µg/cm^2). Cells were treated 4 d after sorting with the mouse recombinant IL-17 (R&D; 421-ML) or mouse recombinant IL-23 (R&D; 1887-ML) for 24 h.

Ex vivo organoid culture

Intestinal organoids were obtained as previously described (Sato et al., 2009). Organoids were treated as follows: mouse recombinant IL-11 (R&D; 418-ML) at 50 ng/ml; mouse recombinant IL-22 (R&D; 582-ML) at 50 ng/ml; IFN-γ (eBiosciences 34-8311-85) at 50 ng/ml for 24 h followed by 16 h of BrdU staining (1/100 dilution of the BrdU labeling reagent; 10373283; Life Technologies). For STAT inhibition, fludarabine was added at 50 mM 24 h before cytokine treatment in WT organoid. For STAT3 depletion, *Stat3$^{fl/fl}$ Villin-cre* organoids were treated with hydroxytamoxifen 24 h before cytokine treatment.

Immunofluorescence staining

Tissues and organoids were labeled as previously described (Disson et al., 2009; Mahe et al., 2013). Intestine or colon was removed from cervical dislocated animals, flushed, and fixed in 4% PFA overnight. Tissues were then washed in PBS and (1) embedded in agarose for 150-µm-thick vibratome section or (2) cryoprotected in sucrose 30%, embedded in optimal cutting temperature compound and nitrogen frozen for 8-µm-thin cryostat section. Organoids were fixed for 30 min in PFA 4% and washed in PBS. For BrdU staining, samples were incubated sequentially in HCl 1N for 10 min at 4°C, HCl 2N for 10 min at room temperature, HCl 2N for 20 min at 37°C, buffered with borate buffer (0.1 M) for 12 min at room temperature, and washed in PBS. Tissues were permeabilized and blocked with 3% BSA in PBS containing 0.4% (thin sections) or 1% (thick sections and organoids) Triton X-100 for at least 1 h. Tissues were then probed with the appropriate primary and secondary antibodies at least 1 h at room temperature or overnight at 4°C. Sections were then mounted in fluorescent mounting medium (Fluoromount G; Beckman Coulter) and dried at 37°C for 30 min. For staining of accessible Ecad, whole mount intestine tissues were labeled with ECCD-2 in PBS BSA 3% as previously described (Nikitas et al., 2011). R12 anti-*Lm* rabbit polyclonal antibody was provided by P. Cossart (Institut Pasteur, Paris, France). Anti-Ki67 was obtained from Abcam. Anti BrdU clone MoBU-1 and anti-Ecad clone ECCD-2, Alexa Fluor 647 Phalloidin, Alexa Fluor 647, Alexa Fluor 488 WGA, Alexa Fluor 546 and 647 goat anti-rabbit, Alexa Fluor 488 and 647 goat anti-rat, and Hoechst 33342 are from Life Technologies.

For 16S staining, tissues were fixed in Carnoy solution for 24 h and then cut, deparaffinized, and treated as previously described (Canny et al., 2006). For Muc2 staining, tissues were fixed in Carnoy solution for 24 h and then cut and deparaffinized. Sections were boiled in 0.01 M citric acid buffer, pH 6, to retrieve the antigens and were permeabilized, blocked, and stained with the anti-MUC2C3, a gift from G. Hansson, Institute of Biomedicine, Gotheburg, Sweden, at 4°C overnight (Johansson et al., 2008).

TUNEL assay was performed according to manufacturer instructions (click-iT Plus TUNEL Assay; Molecular Probes).

Sections were imaged with an inverted Axiobserver or LSM710 confocal Zeiss microscope (20× or 40× oil objectives). BrdU fold increase was calculated by dividing the distance between basal and upper BrdU$^+$ cells by the length of the villus. When indicated, this ratio was normalized by noninfected animals (PBS) of the experiment to normalize for inter-experiments variations. For each experiment, two to three infected animals and one to two control noninfected animals were tested. Experiments were done in duplicate or triplicate. 5–10 villi were counted for each animal. For organoid, BrdU quantification was obtained by measuring the number of BrdU pixels from three-dimensional acquisition with Icy (de Chaumont et al., 2012), divided by the number of crypts (script in Fig. S4 I). All acquisitions and quantifications were done in a blinded manner.

Immunoblot

Tissue was lysed in lysis buffer containing radioimmunoprecipitation assay 1× (Sigma-Aldrich), anti-phosphatase, and anti-protease (Roche). Protein concentration from total protein extracts was quantified using the BCA Protein Assay kit (Thermo Fisher Scientific). 20 µg of protein for each sample was boiled for 5 min in NuPage buffer (Invitrogen) with reducing agent (Invitrogen) and radioimmunoprecipitation assay 1×. Samples were then subjected to SDS-PAGE and transferred onto polyvinylidene fluoride membranes (Millipore). Membranes were activated by absolute ethanol, followed by electro-transfer and saturation with PBS supplemented with 0.1% Tween 20 (Sigma-Aldrich) and 5% non-fat milk. Membranes were incubated with primary antibodies: rabbit anti–phospho-Stat3 (Tyr705; EP2147Y; ab76315; Abcam), mouse anti–phospho-Stat1 (Tyr701; M135; ab29045; Abcam), and mouse anti–β-Actin (clone AC-15; A1978; Sigma-Aldrich). Membranes were washed three times in PBS supplemented with 0.1% Tween 20 (Sigma-Aldrich), incubated with mouse (NA931; GE Healthcare) or rabbit (NA934; GE Healthcare) secondary antibody coupled to peroxidase, washed three times in PBS supplemented with 0.1% Tween 20 (Sigma-Aldrich), and revealed by chemiluminescence with ECL Western blotting detection system (GE Healthcare). Images were acquired and quantified with the PXi4 GeneSys software version 1.3.9.0.

ELISA

IFN-γ, IL-12, and IL-11 were measured with ELISA kits from Abcam from supernatant of intestinal tissue or in vitro cells in culture. Assays were performed according to the manufacturers' instructions.

Histological analysis of DSS-treated mice

DSS was added to drinking water at a concentration of 2.5% 36–50 kD DSS (MP Biomedicals) for seven consecutive days (Chassaing et al., 2014) after *Lm* infection. Histopathological examination of colon was done after fixation of the tissues in PFA 4% and embedding in paraffin. Tissue sections were cut and stained with hematoxylin and eosin. All slides were coded and evaluated in a blinded manner as previously described (Chassaing et al., 2014). In brief, each section was assigned four scores based on the degree of epithelial damage and inflammatory infiltration into the mucosa, submucosa, and muscularis/serosa (0–3). Each of the four scores was multiplied by 1 if the change was focal, 2 if it was patchy, and 3 if it was diffuse. The four individual scores per colon were added, resulting in a total scoring range of 0–36 per mouse.

Statistical analysis

Student's *t* tests, nonparametric Mann-Whitney, or one-way ANOVA tests were routinely used for statistical analysis. Figure legends show the minimum number of mice used in the experiment and the statistical test used. Statistical significance is expressed as follows: *, $P < 0.05$; **, $P < 0.01$; ***, $P < 0.001$; ****, $P < 0.0001$.

Online supplemental material

Fig. S1 shows that *Lm*-induced epithelial cell proliferation is *Lm* strain independent, is not associated to barrier damage, is dose-dependent, and is initiated at the PP level, but not at the villus level. Fig. S2 illustrates STAT3's role on WGA$^+$ GC number decrease and shows that the phenotype is reversible and LLO dependent, but InlA independent. It shows that infected cells are PP CX3CR1$^+$ myeloid cells, which express IL-23 upon infection. Fig. S3 defines the studied gp38$^+$ CD45$^-$ CD31$^-$ stromal cells population. Fig. S4 shows that IFN-γ is expressed by sNK cells in a CX3CR1-dependent, but IL-23–independent, manner. It also shows that STAT-3 phosphorylation in ex vivo organoid is IL-11 or IL-22 dependent, while STAT1 phosphorylation is IFN-γ dependent. It illustrates the script used to quantify BrdU incorporation in organoids. Fig. S5 shows that *Lm*-induced epithelial cell proliferation is observed in colon, where the mucus layer is smaller. It also illustrates the model we propose.

Acknowledgments

We thank the members of the Biology of Infection Unit for their support. We thank Hélène Bierne for her implication in the initial phase of the project, Elena Tomasello and Eric Vivier for helpful discussions, Stéphane Dallongeville for image analysis, Sascha Cording, Morgane Lavina for technical help, and Hana Kammoun for critical reading. We thank Edith Gouin and Pascale Cossart for anti-*Lm* antibodies, Tracy Putoczki for *Il11ra1*$^{-/-}$ mice, Richard Flavell for *Il22*$^{-/-}$ mice, Bernhard Ryffel for *IL23p19*$^{-/-}$ mice, Laure Dumoutier, Jean-Christophe Renauld for anti–IL-22 antibody, and Gunnar C. Hansson for anti-MUC2C3 serum.

This work was financed by Institut Pasteur, Institut National de la Santé et de la Recherche Médicale, Institut Carnot Pasteur Microbes et Santé, LabEx IBEID, the European Research Council grant Invadis, and the Agence Nationale de Recherche Organolist.

The authors declare no competing financial interests.

Author contributions: conceptualization: O. Disson and M. Lecuit; methodology: O. Disson, G. Eberl, J.P. Di Santo, L. Peduto, and M. Lecuit; investigation: O. Disson, C. Blériot, J.-M. Jacob, N. Serafini, G. Gessain, C. Fevre, P. Thouvenot, G. Jouvion, and S. Dulauroy; writing (original draft): O. Disson and M. Lecuit; writing (review and editing): C. Blériot, N. Serafini, G. Eberl, J.P. Di Santo, and L. Peduto; funding acquisition: M. Lecuit; supervision: M. Lecuit; additional mentorship and feedback: G. Eberl, J.P. Di Santo, and L. Peduto.

Submitted: 27 June 2018
Revised: 5 September 2018
Accepted: 28 September 2018

References

Andersson, A., W.J. Dai, J.P. Di Santo, and F. Brombacher. 1998. Early IFN-gamma production and innate immunity during Listeria monocytogenes infection in the absence of NK cells. *J. Immunol.* 161:5600–5606.

Andoh, A., Z. Zhang, O. Inatomi, S. Fujino, Y. Deguchi, Y. Araki, T. Tsujikawa, K. Kitoh, S. Kim-Mitsuyama, A. Takayanagi, et al. 2005. Interleukin-22, a member of the IL-10 subfamily, induces inflammatory responses in colonic subepithelial myofibroblasts. *Gastroenterology.* 129:969–984. https://doi.org/10.1053/j.gastro.2005.06.071

Aparicio-Domingo, P., M. Romera-Hernandez, J.J. Karrich, F. Cornelissen, N. Papazian, D.J. Lindenbergh-Kortleve, J.A. Butler, L. Boon, M.C. Coles, J.N.

Samsom, and T. Cupedo. 2015. Type 3 innate lymphoid cells maintain intestinal epithelial stem cells after tissue damage. *J. Exp. Med.* 212:1783–1791. https://doi.org/10.1084/jem.20150318

Asker, N., M.A. Axelsson, S.O. Olofsson, and G.C. Hansson. 1998. Dimerization of the human MUC2 mucin in the endoplasmic reticulum is followed by a N-glycosylation-dependent transfer of the mono- and dimers to the Golgi apparatus. *J. Biol. Chem.* 273:18857–18863. https://doi.org/10.1074/jbc.273.30.18857

Aychek, T., A. Mildner, S. Yona, K.W. Kim, N. Lampl, S. Reich-Zeliger, L. Boon, N. Yogev, A. Waisman, D.J. Cua, and S. Jung. 2015. IL-23-mediated mononuclear phagocyte crosstalk protects mice from Citrobacter rodentium-induced colon immunopathology. *Nat. Commun.* 6:6525. https://doi.org/10.1038/ncomms7525

Bamba, S., A. Andoh, H. Yasui, J. Makino, S. Kim, and Y. Fujiyama. 2003. Regulation of IL-11 expression in intestinal myofibroblasts: role of c-Jun AP-1- and MAPK-dependent pathways. *Am. J. Physiol. Gastrointest. Liver Physiol.* 285:G529–G538. https://doi.org/10.1152/ajpgi.00050.2003

Barker, N. 2014. Adult intestinal stem cells: critical drivers of epithelial homeostasis and regeneration. *Nat. Rev. Mol. Cell Biol.* 15:19–33. https://doi.org/10.1038/nrm3721

Barker, N., M. van de Wetering, and H. Clevers. 2008. The intestinal stem cell. *Genes Dev.* 22:1856–1864. https://doi.org/10.1101/gad.1674008

Begley, M., C. Kerr, and C. Hill. 2009. Exposure to bile influences biofilm formation by Listeria monocytogenes. *Gut Pathog.* 1:11. https://doi.org/10.1186/1757-4749-1-11

Bonnardel, J., C. Da Silva, S. Henri, S. Tamoutounour, L. Chasson, F. Montañana-Sanchis, J.P. Gorvel, and H. Lelouard. 2015. Innate and adaptive immune functions of peyer's patch monocyte-derived cells. *Cell Reports.* 11:770–784. https://doi.org/10.1016/j.celrep.2015.03.067

Brooling, J.T., J.S. Campbell, C. Mitchell, G.C. Yeoh, and N. Fausto. 2005. Differential regulation of rodent hepatocyte and oval cell proliferation by interferon gamma. *Hepatology.* 41:906–915. https://doi.org/10.1002/hep.20645

Buchon, N., N.A. Broderick, M. Poidevin, S. Pradervand, and B. Lemaitre. 2009. Drosophila intestinal response to bacterial infection: activation of host defense and stem cell proliferation. *Cell Host Microbe.* 5:200–211. https://doi.org/10.1016/j.chom.2009.01.003

Buchon, N., N.A. Broderick, and B. Lemaitre. 2013. Gut homeostasis in a microbial world: insights from Drosophila melanogaster. *Nat. Rev. Microbiol.* 11:615–626. https://doi.org/10.1038/nrmicro3074

Buonocore, S., P.P. Ahern, H.H. Uhlig, I.I. Ivanov, D.R. Littman, K.J. Maloy, and F. Powrie. 2010. Innate lymphoid cells drive interleukin-23-dependent innate intestinal pathology. *Nature.* 464:1371–1375. https://doi.org/10.1038/nature08949

Canny, G., A. Swidsinski, and B.A. McCormick. 2006. Interactions of intestinal epithelial cells with bacteria and immune cells: methods to characterize microflora and functional consequences. *Methods Mol. Biol.* 341:17–35.

Chan, J.M., G. Bhinder, H.P. Sham, N. Ryz, T. Huang, K.S. Bergstrom, and B.A. Vallance. 2013. CD4+ T cells drive goblet cell depletion during Citrobacter rodentium infection. *Infect. Immun.* 81:4649–4658. https://doi.org/10.1128/IAI.00655-13

Charlier, C., C. Fevre, L. Travier, B. Cazenave, H. Bracq-Dieye, J. Podevin, D. Assomany, L. Guilbert, C. Bossard, F. Carpentier, et al. 2014. Listeria monocytogenes-associated biliary tract infections: a study of 12 consecutive cases and review. *Medicine (Baltimore).* 93:e105. https://doi.org/10.1097/MD.0000000000000105

Charlier, C., É. Perrodeau, A. Leclercq, B. Cazenave, B. Pilmis, B. Henry, A. Lopes, M.M. Maury, A. Moura, F. Goffinet, et al. MONALISA study group. 2017. Clinical features and prognostic factors of listeriosis: the MONALISA national prospective cohort study. *Lancet Infect. Dis.* 17:510–519. https://doi.org/10.1016/S1473-3099(16)30521-7

Chassaing, B., J.D. Aitken, M. Malleshappa, and M. Vijay-Kumar. 2014. Dextran sulfate sodium (DSS)-induced colitis in mice. *Curr. Protoc. Immunol.* 104:Unit 15.25.

Chiba, S., T. Nagai, T. Hayashi, Y. Baba, S. Nagai, and S. Koyasu. 2011. Listerial invasion protein internalin B promotes entry into ileal Peyer's patches in vivo. *Microbiol. Immunol.* 55:123–129. https://doi.org/10.1111/j.1348-0421.2010.00292.x

Chudnovskiy, A., A. Mortha, V. Kana, A. Kennard, J.D. Ramirez, A. Rahman, R. Remark, I. Mogno, R. Ng, S. Gnjatic, et al. 2016. Host-Protozoan Interactions Protect from Mucosal Infections through Activation of the Inflammasome. *Cell.* 167:444–456.e14. https://doi.org/10.1016/j.cell.2016.08.076

Collins, J.W., K.M. Keeney, V.F. Crepin, V.A. Rathinam, K.A. Fitzgerald, B.B. Finlay, and G. Frankel. 2014. Citrobacter rodentium: infection, inflammation and the microbiota. *Nat. Rev. Microbiol.* 12:612–623. https://doi.org/10.1038/nrmicro3315

Cuylen, S., C. Blaukopf, A.Z. Politi, T. Müller-Reichert, B. Neumann, I. Poser, J. Ellenberg, A.A. Hyman, and D.W. Gerlich. 2016. Ki-67 acts as a biological surfactant to disperse mitotic chromosomes. *Nature.* 535:308–312. https://doi.org/10.1038/nature18610

de Chaumont, F., S. Dallongeville, N. Chenouard, N. Hervé, S. Pop, T. Provoost, V. Meas-Yedid, P. Pankajakshan, T. Lecomte, Y. Le Montagner, et al. 2012. Icy: an open bioimage informatics platform for extended reproducible research. *Nat. Methods.* 9:690–696. https://doi.org/10.1038/nmeth.2075

Disson, O., S. Grayo, E. Huillet, G. Nikitas, F. Langa-Vives, O. Dussurget, M. Ragon, A. Le Monnier, C. Babinet, P. Cossart, and M. Lecuit. 2008. Conjugated action of two species-specific invasion proteins for fetoplacental listeriosis. *Nature.* 455:1114–1118. https://doi.org/10.1038/nature07303

Disson, O., G. Nikitas, S. Grayo, O. Dussurget, P. Cossart, and M. Lecuit. 2009. Modeling human listeriosis in natural and genetically engineered animals. *Nat. Protoc.* 4:799–810. https://doi.org/10.1038/nprot.2009.66

Dulauroy, S., S.E. Di Carlo, F. Langa, G. Eberl, and L. Peduto. 2012. Lineage tracing and genetic ablation of ADAM12(+) perivascular cells identify a major source of profibrotic cells during acute tissue injury. *Nat. Med.* 18:1262–1270. https://doi.org/10.1038/nm.2848

Eken, A., A.K. Singh, and M. Oukka. 2014. Interleukin 23 in Crohn's disease. *Inflamm. Bowel Dis.* 20:587–595. https://doi.org/10.1097/01.MIB.0000442014.52661.20

El Marjou, F., K.P. Janssen, B.H. Chang, M. Li, V. Hindie, L. Chan, D. Louvard, P. Chambon, D. Metzger, and S. Robine. 2004. Tissue-specific and inducible Cre-mediated recombination in the gut epithelium. *Genesis.* 39:186–193. https://doi.org/10.1002/gene.20042

Ernst, M., S. Thiem, P.M. Nguyen, M. Eissmann, and T.L. Putoczki. 2014. Epithelial gp130/Stat3 functions: an intestinal signaling node in health and disease. *Semin. Immunol.* 26:29–37. https://doi.org/10.1016/j.smim.2013.12.006

Fischer, J., P.J. Klein, M. Vierbuchen, B. Skutta, G. Uhlenbruck, and R. Fischer. 1984. Characterization of glycoconjugates of human gastrointestinal mucosa by lectins. I. Histochemical distribution of lectin binding sites in normal alimentary tract as well as in benign and malignant gastric neoplasms. *J. Histochem. Cytochem.* 32:681–689. https://doi.org/10.1177/32.7.6330198

Frank, D.A., S. Mahajan, and J. Ritz. 1999. Fludarabine-induced immunosuppression is associated with inhibition of STAT1 signaling. *Nat. Med.* 5:444–447. https://doi.org/10.1038/7445

Geng, H., H.F. Bu, F. Liu, L. Wu, K. Pfeifer, P.M. Chou, X. Wang, J. Sun, L. Lu, A. Pandey, et al. 2018. In Inflamed Intestinal Tissues and Epithelial Cells, Interleukin 22 Signaling Increases Expression of H19 Long Noncoding RNA, Which Promotes Mucosal Regeneration. *Gastroenterology.* 155:144–155. https://doi.org/10.1053/j.gastro.2018.03.058

Gessain, G., Y.H. Tsai, L. Travier, M. Bonazzi, S. Grayo, P. Cossart, C. Charlier, O. Disson, and M. Lecuit. 2015. PI3-kinase activation is critical for host barrier permissiveness to Listeria monocytogenes. *J. Exp. Med.* 212:165–183. https://doi.org/10.1084/jem.20141406

Ghilardi, N., N. Kljavin, Q. Chen, S. Lucas, A.L. Gurney, and F.J. De Sauvage. 2004. Compromised humoral and delayed-type hypersensitivity responses in IL-23-deficient mice. *J. Immunol.* 172:2827–2833. https://doi.org/10.4049/jimmunol.172.5.2827

Gibson, D.L., C. Ma, K.S. Bergstrom, J.T. Huang, C. Man, and B.A. Vallance. 2008. MyD88 signalling plays a critical role in host defence by controlling pathogen burden and promoting epithelial cell homeostasis during Citrobacter rodentium-induced colitis. *Cell. Microbiol.* 10:618–631. https://doi.org/10.1111/j.1462-5822.2007.01071.x

Gibson, D.L., M. Montero, M.J. Ropeleski, K.S. Bergstrom, C. Ma, S. Ghosh, H. Merkens, J. Huang, L.E. Månsson, H.P. Sham, et al. 2010. Interleukin-11 reduces TLR4-induced colitis in TLR2-deficient mice and restores intestinal STAT3 signaling. *Gastroenterology.* 139:1277–1288. https://doi.org/10.1053/j.gastro.2010.06.057

Gonneaud, A., N. Turgeon, F. Boudreau, N. Perreault, N. Rivard, and C. Asselin. 2016. Distinct Roles for Intestinal Epithelial Cell-Specific Hdac1 and Hdac2 in the Regulation of Murine Intestinal Homeostasis. *J. Cell. Physiol.* 231:436–448. https://doi.org/10.1002/jcp.25090

Graham, A.C., K.D. Carr, A.N. Sieve, M. Indramohan, T.J. Break, and R.E. Berg. 2011. IL-22 production is regulated by IL-23 during Listeria monocytogenes infection but is not required for bacterial clearance or tissue protection. *PLoS One.* 6:e17171. https://doi.org/10.1371/journal.pone.0017171

Grivennikov, S.I., K. Wang, D. Mucida, C.A. Stewart, B. Schnabl, D. Jauch, K. Taniguchi, G.Y. Yu, C.H. Osterreicher, K.E. Hung, et al. 2012. Adenoma-linked barrier defects and microbial products drive IL-23/IL-17-me-

diated tumour growth. *Nature.* 491:254–258. https://doi.org/10.1038/nature11465

Gustafsson, J.K., N. Navabi, A.M. Rodriguez-Piñeiro, A.H. Alomran, P. Premaratne, H.R. Fernandez, D. Banerjee, H. Sjövall, G.C. Hansson, and S.K. Lindén. 2013. Dynamic changes in mucus thickness and ion secretion during Citrobacter rodentium infection and clearance. *PLoS One.* 8:e84430. https://doi.org/10.1371/journal.pone.0084430

Hamada, S., M. Umemura, T. Shiono, K. Tanaka, A. Yahagi, M.D. Begum, K. Oshiro, Y. Okamoto, H. Watanabe, K. Kawakami, et al. 2008. IL-17A produced by gammadelta T cells plays a critical role in innate immunity against listeria monocytogenes infection in the liver. *J. Immunol.* 181:3456–3463. https://doi.org/10.4049/jimmunol.181.5.3456

Hamon, M.A., D. Ribet, F. Stavru, and P. Cossart. 2012. Listeriolysin O: the Swiss army knife of Listeria. *Trends Microbiol.* 20:360–368. https://doi.org/10.1016/j.tim.2012.04.006

Harty, J.T., and M.J. Bevan. 1995. Specific immunity to Listeria monocytogenes in the absence of IFN gamma. *Immunity.* 3:109–117. https://doi.org/10.1016/1074-7613(95)90163-9

Hugot, J.P., C. Alberti, D. Berrebi, E. Bingen, and J.P. Cézard. 2003. Crohn's disease: the cold chain hypothesis. *Lancet.* 362:2012–2015. https://doi.org/10.1016/S0140-6736(03)15024-6

Indra, A.K., X. Warot, J. Brocard, J.M. Bornert, J.H. Xiao, P. Chambon, and D. Metzger. 1999. Temporally-controlled site-specific mutagenesis in the basal layer of the epidermis: comparison of the recombinase activity of the tamoxifen-inducible Cre-ER(T) and Cre-ER(T2) recombinases. *Nucleic Acids Res.* 27:4324–4327. https://doi.org/10.1093/nar/27.22.4324

Ishida, Y., T. Hayashi, T. Goto, A. Kimura, S. Akimoto, N. Mukaida, and T. Kondo. 2008. Essential involvement of CX3CR1-mediated signals in the bactericidal host defense during septic peritonitis. *J. Immunol.* 181:4208–4218. https://doi.org/10.4049/jimmunol.181.6.4208

Iwai, H., M. Kim, Y. Yoshikawa, H. Ashida, M. Ogawa, Y. Fujita, D. Muller, T. Kirikae, P.K. Jackson, S. Kotani, and C. Sasakawa. 2007. A bacterial effector targets Mad2L2, an APC inhibitor, to modulate host cell cycling. *Cell.* 130:611–623. https://doi.org/10.1016/j.cell.2007.06.043

Jensen, V.B., J.T. Harty, and B.D. Jones. 1998. Interactions of the invasive pathogens Salmonella typhimurium, Listeria monocytogenes, and Shigella flexneri with M cells and murine Peyer's patches. *Infect. Immun.* 66:3758–3766.

Johansson, M.E., M. Phillipson, J. Petersson, A. Velcich, L. Holm, and G.C. Hansson. 2008. The inner of the two Muc2 mucin-dependent mucus layers in colon is devoid of bacteria. *Proc. Natl. Acad. Sci. USA.* 105:15064–15069. https://doi.org/10.1073/pnas.0803124105

Jung, S., J. Aliberti, P. Graemmel, M.J. Sunshine, G.W. Kreutzberg, A. Sher, and D.R. Littman. 2000. Analysis of fractalkine receptor CX(3)CR1 function by targeted deletion and green fluorescent protein reporter gene insertion. *Mol. Cell. Biol.* 20:4106–4114. https://doi.org/10.1128/MCB.20.11.4106-4114.2000

Klose, C.S., E.A. Kiss, V. Schwierzeck, K. Ebert, T. Hoyler, Y. d'Hargues, N. Göppert, A.L. Croxford, A. Waisman, Y. Tanriver, and A. Diefenbach. 2013. A T-bet gradient controls the fate and function of CCR6-RORγt+ innate lymphoid cells. *Nature.* 494:261–265. https://doi.org/10.1038/nature11813

Kuipers, E.J., W.M. Grady, D. Lieberman, T. Seufferlein, J.J. Sung, P.G. Boelens, C.J. van de Velde, and T. Watanabe. 2015. Colorectal cancer. *Nat. Rev. Dis. Primers.* 1:15065. https://doi.org/10.1038/nrdp.2015.65

Lecuit, M., S. Vandormael-Pournin, J. Lefort, M. Huerre, P. Gounon, C. Dupuy, C. Babinet, and P. Cossart. 2001. A transgenic model for listeriosis: role of internalin in crossing the intestinal barrier. *Science.* 292:1722–1725. https://doi.org/10.1126/science.1059852

Lecuit, M., J.L. Sonnenburg, P. Cossart, and J.I. Gordon. 2007. Functional genomic studies of the intestinal response to a foodborne enteropathogen in a humanized gnotobiotic mouse model. *J. Biol. Chem.* 282:15065–15072. https://doi.org/10.1074/jbc.M610926200

Lindemans, C.A., M. Calafiore, A.M. Mertelsmann, M.H. O'Connor, J.A. Dudakov, R.R. Jenq, E. Velardi, L.F. Young, O.M. Smith, G. Lawrence, et al. 2015. Interleukin-22 promotes intestinal-stem-cell-mediated epithelial regeneration. *Nature.* 528:560–564. https://doi.org/10.1038/nature16460

Liu, Y., H.J. van Kruiningen, A.B. West, R.W. Cartun, A. Cortot, and J.F. Colombel. 1995. Immunocytochemical evidence of Listeria, Escherichia coli, and Streptococcus antigens in Crohn's disease. *Gastroenterology.* 108:1396–1404. https://doi.org/10.1016/0016-5085(95)90687-8

Longman, R.S., G.E. Diehl, D.A. Victorio, J.R. Huh, C. Galan, E.R. Miraldi, A. Swaminath, R. Bonneau, E.J. Scherl, and D.R. Littman. 2014. CX_3CR1^+ mononuclear phagocytes support colitis-associated innate lymphoid cell production of IL-22. *J. Exp. Med.* 211:1571–1583. https://doi.org/10.1084/jem.20140678

Mahapatro, M., S. Foersch, M. Hefele, G.W. He, E. Giner-Ventura, T. Mchedlidze, M. Kindermann, S. Vetrano, S. Danese, C. Günther, et al. 2016. Programming of Intestinal Epithelial Differentiation by IL-33 Derived from Pericryptal Fibroblasts in Response to Systemic Infection. *Cell Reports.* 15:1743–1756. https://doi.org/10.1016/j.celrep.2016.04.049

Mahe, M.M., E. Aihara, M.A. Schumacher, Y. Zavros, M.H. Montrose, M.A. Helmrath, T. Sato, and N.F. Shroyer. 2013. Establishment of Gastrointestinal Epithelial Organoids. *Curr. Protoc. Mouse Biol.* 3:217–240. https://doi.org/10.1002/9780470942390.mo130179

Manta, C., E. Heupel, K. Radulovic, V. Rossini, N. Garbi, C.U. Riedel, and J.H. Niess. 2013. CX(3)CR1(+) macrophages support IL-22 production by innate lymphoid cells during infection with Citrobacter rodentium. *Mucosal Immunol.* 6:177–188. https://doi.org/10.1038/mi.2012.61

Mimuro, H., T. Suzuki, J. Tanaka, M. Asahi, R. Haas, and C. Sasakawa. 2002. Grb2 is a key mediator of helicobacter pylori CagA protein activities. *Mol. Cell.* 10:745–755. https://doi.org/10.1016/S1097-2765(02)00681-0

Miranda-Bautista, J., C. Padilla-Suárez, E. Bouza, P. Muñoz, L. Menchén, and I. Marín-Jiménez. 2014. Listeria monocytogenes infection in inflammatory bowel disease patients: case series and review of the literature. *Eur. J. Gastroenterol. Hepatol.* 26:1247–1252. https://doi.org/10.1097/MEG.0000000000000188

Nandurkar, H.H., L. Robb, D. Tarlinton, L. Barnett, F. Köntgen, and C.G. Begley. 1997. Adult mice with targeted mutation of the interleukin-11 receptor (IL11Ra) display normal hematopoiesis. *Blood.* 90:2148–2159.

Ng, S.C., C.N. Bernstein, M.H. Vatn, P.L. Lakatos, E.V. Loftus Jr., C. Tysk, C. O'Morain, B. Moum, and J.F. Colombel. Epidemiology and Natural History Task Force of the International Organization of Inflammatory Bowel Disease (IOIBD). 2013. Geographical variability and environmental risk factors in inflammatory bowel disease. *Gut.* 62:630–649. https://doi.org/10.1136/gutjnl-2012-303661

Nikitas, G., C. Deschamps, O. Disson, T. Niault, P. Cossart, and M. Lecuit. 2011. Transcytosis of Listeria monocytogenes across the intestinal barrier upon specific targeting of goblet cell accessible E-cadherin. *J. Exp. Med.* 208:2263–2277. https://doi.org/10.1084/jem.20110560

Niv, Y. 2016. Mucin Genes Expression in the Intestine of Crohn's Disease Patients: a Systematic Review and Meta-analysis. *J. Gastrointestin. Liver Dis.* 25:351–357.

Nowarski, R., R. Jackson, N. Gagliani, M.R. de Zoete, N.W. Palm, W. Bailis, J.S. Low, C.C. Harman, M. Graham, E. Elinav, and R.A. Flavell. 2015. Epithelial IL-18 Equilibrium Controls Barrier Function in Colitis. *Cell.* 163:1444–1456. https://doi.org/10.1016/j.cell.2015.10.072

Okayasu, I., S. Hatakeyama, M. Yamada, T. Ohkusa, Y. Inagaki, and R. Nakaya. 1990. A novel method in the induction of reliable experimental acute and chronic ulcerative colitis in mice. *Gastroenterology.* 98:694–702. https://doi.org/10.1016/0016-5085(90)90290-H

Opal, S.M., J.C. Keith, J.E. Palardy, and N. Parejo. 2000. Recombinant human interleukin-11 has anti-inflammatory actions yet does not exacerbate systemic Listeria infection. *J. Infect. Dis.* 181:754–756. https://doi.org/10.1086/315247

Owens, B.M., and A. Simmons. 2013. Intestinal stromal cells in mucosal immunity and homeostasis. *Mucosal Immunol.* 6:224–234. https://doi.org/10.1038/mi.2012.125

Peduto, L., S. Dulauroy, M. Lochner, G.F. Späth, M.A. Morales, A. Cumano, and G. Eberl. 2009. Inflammation recapitulates the ontogeny of lymphoid stromal cells. *J. Immunol.* 182:5789–5799. https://doi.org/10.4049/jimmunol.0803974

Pickert, G., C. Neufert, M. Leppkes, Y. Zheng, N. Wittkopf, M. Warntjen, H.A. Lehr, S. Hirth, B. Weigmann, S. Wirtz, et al. 2009. STAT3 links IL-22 signaling in intestinal epithelial cells to mucosal wound healing. *J. Exp. Med.* 206:1465–1472. https://doi.org/10.1084/jem.20082683

Putoczki, T., and M. Ernst. 2010. More than a sidekick: the IL-6 family cytokine IL-11 links inflammation to cancer. *J. Leukoc. Biol.* 88:1109–1117. https://doi.org/10.1189/jlb.0410226

Putoczki, T.L., S. Thiem, A. Loving, R.A. Busuttil, N.J. Wilson, P.K. Ziegler, P.M. Nguyen, A. Preaudet, R. Farid, K.M. Edwards, et al. 2013. Interleukin-11 is the dominant IL-6 family cytokine during gastrointestinal tumorigenesis and can be targeted therapeutically. *Cancer Cell.* 24:257–271. https://doi.org/10.1016/j.ccr.2013.06.017

Rakoff-Nahoum, S., J. Paglino, F. Eslami-Varzaneh, S. Edberg, and R. Medzhitov. 2004. Recognition of commensal microflora by toll-like receptors is

required for intestinal homeostasis. *Cell.* 118:229–241. https://doi.org/10.1016/j.cell.2004.07.002

Reynders, A., N. Yessaad, T.P. Vu Manh, M. Dalod, A. Fenis, C. Aubry, G. Nikitas, B. Escalière, J.C. Renauld, O. Dussurget, et al. 2011. Identity, regulation and in vivo function of gut NKp46+RORγt+ and NKp46+RORγt- lymphoid cells. *EMBO J.* 30:2934–2947. https://doi.org/10.1038/emboj.2011.201

Sansonetti, P.J., G. Tran Van Nhieu, and C. Egile. 1999. Rupture of the intestinal epithelial barrier and mucosal invasion by Shigella flexneri. *Clin. Infect. Dis.* 28:466–475. https://doi.org/10.1086/515150

Sato, T., R.G. Vries, H.J. Snippert, M. van de Wetering, N. Barker, D.E. Stange, J.H. van Es, A. Abo, P. Kujala, P.J. Peters, and H. Clevers. 2009. Single Lgr5 stem cells build crypt-villus structures in vitro without a mesenchymal niche. *Nature.* 459:262–265. https://doi.org/10.1038/nature07935

Satoh-Takayama, N., C.A. Vosshenrich, S. Lesjean-Pottier, S. Sawa, M. Lochner, F. Rattis, J.J. Mention, K. Thiam, N. Cerf-Bensussan, O. Mandelboim, et al. 2008. Microbial flora drives interleukin 22 production in intestinal NKp46+ cells that provide innate mucosal immune defense. *Immunity.* 29:958–970. https://doi.org/10.1016/j.immuni.2008.11.001

Sheridan, B.S., P.A. Romagnoli, Q.M. Pham, H.H. Fu, F. Alonzo III, W.D. Schubert, N.E. Freitag, and L. Lefrançois. 2013. γδ T cells exhibit multifunctional and protective memory in intestinal tissues. *Immunity.* 39:184–195. https://doi.org/10.1016/j.immuni.2013.06.015

Smith, D.G., S.C. Mitchell, T. Nash, and S. Rhind. 2000. Gamma interferon influences intestinal epithelial hyperplasia caused by Lawsonia intracellularis infection in mice. *Infect. Immun.* 68:6737–6743. https://doi.org/10.1128/IAI.68.12.6737-6743.2000

Sommer, F., and F. Bäckhed. 2013. The gut microbiota--masters of host development and physiology. *Nat. Rev. Microbiol.* 11:227–238. https://doi.org/10.1038/nrmicro2974

Songhet, P., M. Barthel, B. Stecher, A.J. Müller, M. Kremer, G.C. Hansson, and W.D. Hardt. 2011. Stromal IFN-γR-signaling modulates goblet cell function during Salmonella Typhimurium infection. *PLoS One.* 6:e22459. https://doi.org/10.1371/journal.pone.0022459

Stzepourginski, I., G. Eberl, and L. Peduto. 2015. An optimized protocol for isolating lymphoid stromal cells from the intestinal lamina propria. *J. Immunol. Methods.* 421:14–19. https://doi.org/10.1016/j.jim.2014.11.013

Stzepourginski, I., G. Nigro, J.M. Jacob, S. Dulauroy, P.J. Sansonetti, G. Eberl, and L. Peduto. 2017. CD34+ mesenchymal cells are a major component of the intestinal stem cells niche at homeostasis and after injury. *Proc. Natl. Acad. Sci. USA.* 114:E506–E513. https://doi.org/10.1073/pnas.1620059114

Swaminathan, B., and P. Gerner-Smidt. 2007. The epidemiology of human listeriosis. *Microbes Infect.* 9:1236–1243. https://doi.org/10.1016/j.micinf.2007.05.011

Takeda, K., T. Kaisho, N. Yoshida, J. Takeda, T. Kishimoto, and S. Akira. 1998. Stat3 activation is responsible for IL-6-dependent T cell proliferation through preventing apoptosis: generation and characterization of T cell-specific Stat3-deficient mice. *J. Immunol.* 161:4652–4660.

Tsai, Y.H., O. Disson, H. Bierne, and M. Lecuit. 2013. Murinization of internalin extends its receptor repertoire, altering Listeria monocytogenes cell tropism and host responses. *PLoS Pathog.* 9:e1003381. https://doi.org/10.1371/journal.ppat.1003381

Van der Sluis, M., B.A. De Koning, A.C. De Bruijn, A. Velcich, J.P. Meijerink, J.B. Van Goudoever, H.A. Büller, J. Dekker, I. Van Seuningen, I.B. Renes, and A.W. Einerhand. 2006. Muc2-deficient mice spontaneously develop colitis, indicating that MUC2 is critical for colonic protection. *Gastroenterology.* 131:117–129. https://doi.org/10.1053/j.gastro.2006.04.020

Varol, C., A. Vallon-Eberhard, E. Elinav, T. Aychek, Y. Shapira, H. Luche, H.J. Fehling, W.D. Hardt, G. Shakhar, and S. Jung. 2009. Intestinal lamina propria dendritic cell subsets have different origin and functions. *Immunity.* 31:502–512. https://doi.org/10.1016/j.immuni.2009.06.025

Velcich, A., W. Yang, J. Heyer, A. Fragale, C. Nicholas, S. Viani, R. Kucherlapati, M. Lipkin, K. Yang, and L. Augenlicht. 2002. Colorectal cancer in mice genetically deficient in the mucin Muc2. *Science.* 295:1726–1729. https://doi.org/10.1126/science.1069094

Whitfield, M.L., L.K. George, G.D. Grant, and C.M. Perou. 2006. Common markers of proliferation. *Nat. Rev. Cancer.* 6:99–106. https://doi.org/10.1038/nrc1802

Zenewicz, L.A., G.D. Yancopoulos, D.M. Valenzuela, A.J. Murphy, M. Karow, and R.A. Flavell. 2007. Interleukin-22 but not interleukin-17 provides protection to hepatocytes during acute liver inflammation. *Immunity.* 27:647–659. https://doi.org/10.1016/j.immuni.2007.07.023

Zheng, Y., P.A. Valdez, D.M. Danilenko, Y. Hu, S.M. Sa, Q. Gong, A.R. Abbas, Z. Modrusan, N. Ghilardi, F.J. de Sauvage, and W. Ouyang. 2008. Interleukin-22 mediates early host defense against attaching and effacing bacterial pathogens. *Nat. Med.* 14:282–289. https://doi.org/10.1038/nm1720